Clim Dyn (2015) 45:3183–3203
DOI 10.1007/s00382-015-2533-1

A correlated shortening of the North and South American monsoon seasons in the past few decades

Paola A. Arias · Rong Fu · Carolina Vera · Maisa Rojas

Received: 29 September 2014 / Accepted: 16 February 2015 / Published online: 25 February 2015

Abstract Our observational analysis shows that the wet seasons of the American monsoon systems have shortened since 1978 due to correlated earlier retreats of the North American monsoon (NAM) and late onsets of the southern Amazon wet season, an important part of the South American monsoon (SAM). These changes are related to the combination of the global sea surface temperature (SST) warming mode, the El Niño-Southern Oscillation (ENSO), the Atlantic Multidecadal Oscillation (AMO), the westward shift of the North Atlantic subtropical high (NASH), and the enhancement of Pacific South American and Pacific North American wave train patterns, which induces variations of the regional circulation at interannual and decadal scales. The joint contributions from these forcing factors are associated with a stronger and more equatorward regional Hadley cell, which enhances convergence towards the equator, strengthening and possibly delaying the retreat of the tropical part of the NAM. This in turn accelerates the demise of the northern NAM and delays the reversal of the cross-equatorial flow over South America, reducing moisture transport to the SAM and delaying its onset. In addition, the thermodynamic response to warming appears to cause local drier land conditions over both regions, reinforcing the observed changes in these monsoons. Although previous studies have identified the isolated influence of the regional Hadley cell, ENSO, AMO, global SST warming, and NASH on the NAM, the correlated changes between NAM and SAM through variations of the cross-equatorial flow had not been established before.

Keywords Southern Amazon wet season · North American monsoon · South American monsoon · North Atlantic subtropical high · Cross-equatorial flow · Global warming

P. A. Arias (✉)
Grupo de Ingeniería y Gestión Ambiental (GIGA), Escuela Ambiental, Facultad de Ingeniería, Universidad de Antioquia, Calle 67 # 53-108, Bloque 20, Oficina 441, A. A. 1226, Medellín, Colombia
e-mail: paola.arias@udea.edu.co

P. A. Arias · M. Rojas
Departamento de Geofísica, Universidad de Chile, Santiago, Chile

R. Fu
Department of Geological Sciences, The University of Texas at Austin, Austin, TX, USA

C. Vera
Centro de Investigaciones del Mar y la Atmósfera, CONICET-UBA, DCAO/FCEN, UMI, IFAECI/CNRS, Buenos Aires, Argentina

1 Introduction

Summer precipitation over the tropical portions of both North and South America contributes more than half of the total annual precipitation to these regions (e.g. Figueroa and Nobre 1990; Higgins et al. 1997). Such rainfall amounts are produced by the monsoon systems that take place over both continents. The regions affected by the North American monsoon (NAM) are among the zones with most rapidly growing population of the United States (US) and Mexico whereas the South American monsoon (SAM) affects large and highly populated areas of Brazil, Argentina, Bolivia, and Paraguay. The circulation patterns established by these systems control the summer weather over these regions and have important socio-economic implications.

Recent studies have suggested a shortening of both NAM and SAM duration in the past few decades. In particular, Arias et al. (2012) suggest an increased frequency of weak and early-retreat NAM events after 1990 due to the combination of three main factors: (1) the positive phase of the AMO, (2) the northward shift of the subtropical jets over North America, and (3) the westward shift of the North Atlantic surface high (NASH) observed after 1978 (Li et al. 2011). Another study by Fu et al. (2013) has shown a lengthening of the dry season and a delayed wet season onset over the southern Amazon since 1978, as a consequence of increased atmospheric stability and a poleward shift of the Southern Hemisphere subtropical jet. However, it is not clear whether such shortening of the NAM and SAM is independent of each other, or they are related events. If they were related, what would cause such a relationship? This study aims to explore these questions.

Climatologically, the NAM rainfall starts by early to mid June over southwestern Mexico and advances to northwestern Mexico and the southwestern (SW) US by July (e.g., Douglas et al. 1993; Higgins et al. 1997; Barlow et al. 1998). During this evolution, large amounts of moisture are transported from the Gulf of California (at surface) and the Gulf of Mexico (at mid-levels in the atmosphere) to the monsoon region (Higgins et al. 1997; Adams and Comrie 1997). Once the NAM is fully developed, precipitation amounts are larger over the Mexican domain (influenced by abundant tropical moisture and thunderstorms) and lighter over the SW US (influenced by mid-latitude effects and gulf surges) (Higgins et al. 1999; Stensrud et al. 1995). The mature phase of the NAM coincides with the peak of the dry season over the southern Amazon, which is an important part of the SAM. The NAM retreats southward from the SW US and western Mexico to Central America during September–October, then into northern South America by November–December. During the same period, the wet season spreads quickly from the equatorial western Amazon to the east and southeast. By October, monsoon activity starts over the Amazon and the Brazilian highlands, extending to southeastern Brazil by November (e.g., Zhou and Lau 1998; Vera et al. 2006, 2013; Marengo et al. 2010 and references cited therein). The mature phase of the SAM occurs from late November to late February, when large amounts of precipitation fall across the Amazon basin. The South Atlantic Convergence Zone also forms as a result of combined continental heating, transient moisture transport, and extratropical frontal systems (Figueroa et al. 1995; Lenters and Cook 1996; Liebmann et al. 1999). Throughout this evolution, moisture is transported into the Amazon by a northerly low-level cross-equatorial flow (Wang and Fu 2002) and from the Amazon to the La Plata basins by the South American Low-level jet (e.g. Berbery and Barros 2002). During March to May, the regions of large precipitation over subtropical and tropical South America reduce in size and migrate slowly toward the equator, in association with a southerly regime of the low-level cross-equatorial flow, indicating the retreat of the SAM and the transition towards a NAM regime.

The year-to-year variability of the American monsoons is modulated by both local changes of sea surface temperatures (SSTs) and by the remote influence of different large-scale ocean–atmosphere variability modes on the regional circulation anomalies (Vera et al. 2006 and references therein). The NAM is affected at interannual and interdecadal timescales by the Pacific Decadal Oscillation (PDO), the El Niño Southern Oscillation (ENSO), the Atlantic Multidecadal Oscillation (AMO), and the Arctic Oscillation (e.g., Higgins and Shi 2000; Enfield et al. 2001; Castro et al. 2001, 2007; Schubert et al. 2004; McCabe et al. 2004; Seager et al. 2005; Hu and Feng 2008, 2010; Kushnir et al. 2010; Mo 2010; Arias et al. 2012). Furthermore, a recent study by Lee et al. (2014) identified an increased activity of the Western North Pacific summer monsoon since mid-1990s, which induces decadal changes on the other northern hemispheric monsoons, including the NAM. The changes are attributed to the increase of central Pacific type of ENSO, and are exerted through anomalous wave trains. Rainfall over the SAM is influenced by Atlantic (SSTAs; Mechoso et al. 1990; Giannini et al. 2001; Chiessi et al. 2009; Apaestegui et al. 2014) and Pacific SST anomalies (Moura and Shukla 1981; Pisciottano et al. 1994; Grimm et al. 1998; Nogues-Paegle and Mo 2002; Marengo et al. 2004; Grimm 2011 and references therein). Modulations of ENSO impact onto South America summer climate by PDO activity has also been documented (e.g. da Silva et al. 2011). Moreover, after the early 2000s, a weakening of the interannual variability of the tropical Pacific has been identified (Hu et al. 2013), which seems to have influenced precipitation variability at both tropical and subtropical South America. In addition, the poleward shift of the subtropical jet over South America, caused by the warming of the tropical central Pacific (Ding et al. 2012), appears to be a main contributor to the delay of the wet season over the southern Amazon (Fu et al. 2013). However, whether these oceanic variability and changes contribute to the correlated changes between NAM retreat and SAM onset was not addressed in these studies.

Large-scale circulations associated with teleconnection patterns such as the Pacific-North American (PNA) and the Pacific-South American (PSA) patterns also induce monsoon variability over both continents. The PNA pattern in winter and spring is followed by an enhanced upper-troposphere NAM anticyclone and rainfall in summer (Higgins et al. 1998), whereas the PSA pattern causes upper-troposphere anticyclonic (cyclonic) anomalies at the extra-tropics that reduce (enhance) precipitation over southeastern South America (e.g. Grimm et al. 2000). Although both patterns are mainly influenced by ENSO, other independent factors also contribute to their variability (Higgins et al. 2000b; Vera et al. 2004; Munoz et al. 2010). Particularly, PSA pattern is influenced, besides ENSO, by the variability of tropical Indian and Pacific SSTs (Mo 2000). In addition, land surface-related processes such as evaporation and recycling (Anderson et al. 2004; Li and Fu 2004; Zhu et al. 2007), synoptic-scale transient activity (Gonzalez et al. 2007; Douglas and Englehart 2007), and cold-air incursions (Li and Fu 2006; Raia and Cavalcanti 2008) also modulate monsoon rainfall variability over the Americas.

We will investigate the above-discussed processes in order to explore whether there might be common causes for the earlier NAM demise and late SAM onset. A clarification for such causes is particularly relevant to better understand and simulate the unified view of the American monsoon systems, advocated by the World Climate Research Programme/Climate Variability and Predictability/Variability of the American Monsoon Systems (WCRP/CLIVAR/VAMOS) program (Vera et al. 2006). An initial discussion by Fu et al. (2014) suggests that the onsets of the American monsoons are mainly driven by seasonal variability of SSTs over the adjacent oceans, regional land surface heating, and associated circulation changes, instead of remote influence through inter-monsoon connection; however, these monsoon onsets could influence the reversal of the large-scale cross-equatorial flow, possibly affecting the decaying monsoon on the other hemisphere.

This paper is organized in five sections. Section 2 describes the data and the methodology implemented. Section 3 analyzes surface and upper-level circulation changes during the long-transition seasons and their associated changes in convection and SSTs, as well as the influence of the global SST warming, ENSO, and AMO modes, and the NASH westward shift onto the moisture transport to the Amazon and wave train patterns. Section 4 briefly discusses the possible influence of the increasing atmospheric CO_2 concentration in the climate system on the changes in the American monsoons timing. Finally, Sect. 5 presents the main conclusions.

2 Data and methodology

This paper analyzes surface and upper-troposphere circulation, rain rate anomalies, and SSTAs during the transition season between the NAM and SAM systems, which typically occurs from August to October. The transition season between both monsoons was defined as the period between the NAM retreat date and the southern Amazon wet season onset date for each year during the period 1978–2009. The onset/retreat dates were obtained over the spatial domains of the NAM and the southern Amazon, defined by Arias et al. (2012) and Fu et al. (2013), respectively. The NAM domain corresponds to northwestern Mexico whereas the southern Amazon domain corresponds to the region delimited by 50°W–70°W, 15°S–5°S (Fig. 1a). Daily rainfall data were converted to pentad values (i.e., 5 days average) before obtaining onset/retreat dates. The definition of the onset/retreat dates of the American monsoon systems follows Li and Fu's (2004) methodology, which considers both an objectively defined rain rate threshold and the persistence in time. Thus, the onset (retreat) date was defined as the pentad before which the rain rate was less (more) than the climatological annual mean rain rate during 6 out of 8 preceding pentads and after which the rain rate was greater (lower) than the climatological annual mean rain rate during 6 out of 8 subsequent pentads. When these thresholds did not allow identifying the monsoon onset (or retreat) date for a specific year, the duration threshold was relaxed from 6 to 5 consecutive pentads (Arias et al. 2012).

To obtain the southern Amazon wet season onset dates, we used two different rainfall datasets over South America: (1) the 1-degree grid rain gauge daily precipitation from the National Oceanic and Atmospheric Administration (NOAA) Climate Prediction Center (CPC) available during January 1978- December 2007 (Silva et al. 2007; hereafter referred to as Silva data) and (2) the NOAA Climate Diagnostics Center (CDC) daily precipitation gridded data version SA24 available from January 1940 to December 2011 (Liebmann and Allured 2005; hereafter referred to as SA24 data). Following Fu et al. (2013), we merged the two daily rainfall data averaging them over each map cell for the period 1979–2007 when they overlap, and using SA24 for the period 2008–2011. This merged daily rainfall data was constructed in order to reduce the differences detected between both datasets in the areas covered by raingauges (Fu et al. 2013). NAM retreat dates were obtained from the NOAA CPC 1° grid daily precipitation over the US and Mexico (hereafter referred to as CPC US-Mex data). This dataset is described by Higgins et al. (1999, 2000a) and is available during 1940–2009. To match the record period of the merged daily rainfall dataset over South America, only data during 1978–2009 were used.

The confidence intervals and significance levels for the linear trends, computed from the resulting onset/retreat dates and transition season length, were determined based on the effective sample size and the t test (Santer et al. 2000). The linear trend significances are also confirmed by the non-parametric Mann–Kendall test with Sen's statistics (Sen 1968).

We analyzed the changes in lower and upper troposphere circulation, as well as surface dryness conditions, compositing different variables during long and short-transition seasons. Dryness land conditions were represented by the Bowen Ratio (BR), defined as the ratio between sensible and latent heat fluxes. Therefore, daily 2.5° grid data for

Fig. 1 **a** Regions considered for this study: southern Amazon domain (*black*), NAM domain (*red*), and V-Index domain (*blue*). **b** NAM retreat date (*red*) and southern Amazon wet season onset date (*black*) during 1978–2009. NAM retreat and southern Amazon wet season onset dates are significantly correlated at $P < 0.05$. **c** NAM onset date (*red*) and southern Amazon wet season retreat date (*black*). **d** Length of the transition season from NAM to southern Amazon wet season. Linear trend for the transition season length (*dashed line*) and its confidence interval are statistically significant at $P < 0.06$ using the Santer et al. (2000) test. *Solid lines* represent the lower and upper level defined to distinguish short and long-transition seasons, respectively. *Asterisks* (*diamonds*) correspond to short (long) transition seasons

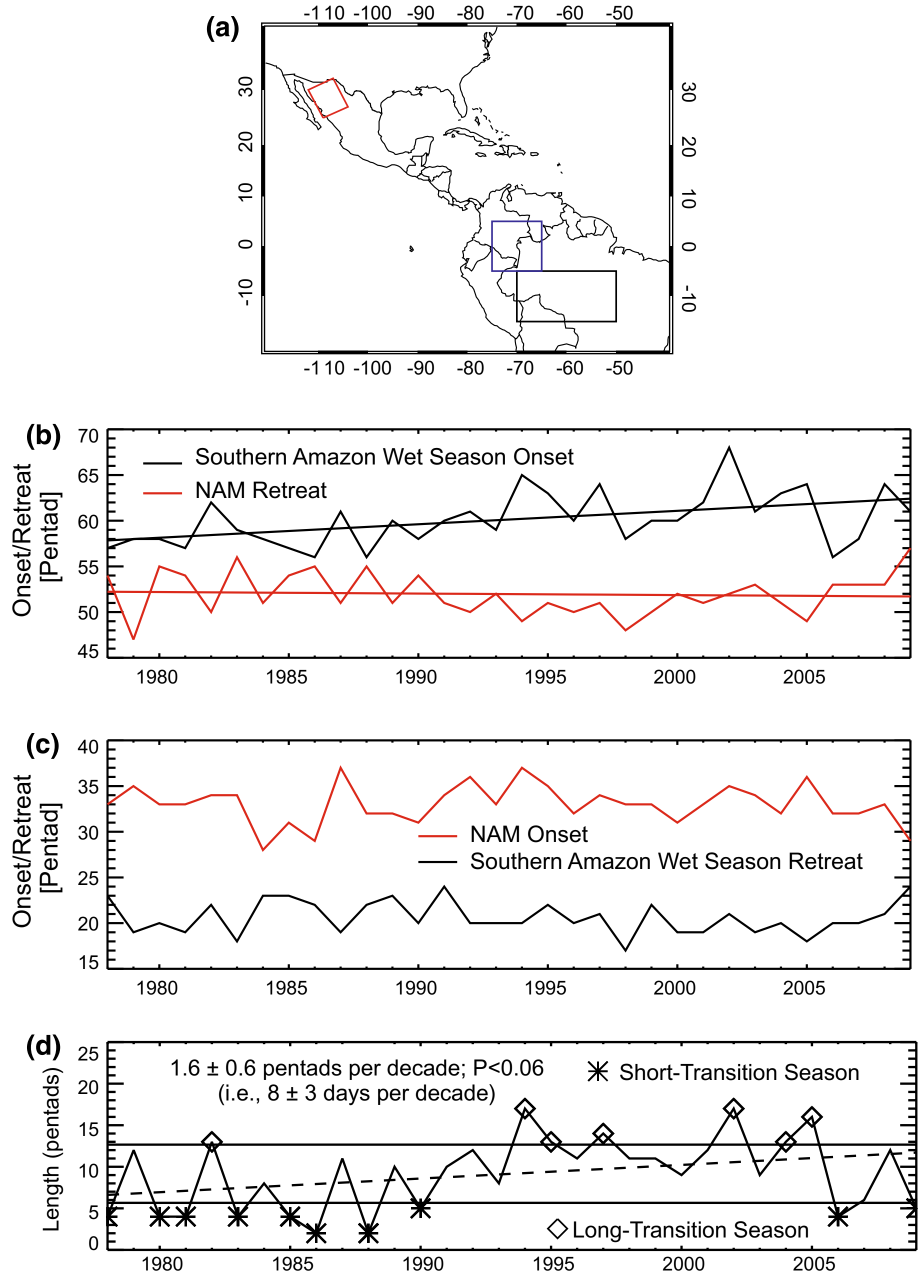

latent and sensible heat fluxes, geopotential height, horizontal winds, vertical velocity, and streamfunction at different pressure levels were obtained from the National Center for Environmental Project-National Center for Atmospheric Research (NCEP-NCAR) Reanalysis (Kalnay et al. 1996) from 1978 to present. We also used monthly mean rain rate from the Global Precipitation Climatology Project (GPCP, Adler et al. 2003), available after 1979 and provided at a 2.5° resolution by the NOAA/ESRL/PSD (http://www.esr.noaa.gov/psd/).

Extended reconstructed monthly mean SSTs from the NOAA Climate Diagnostic Center (CDC) (Reynolds 1988) were used with a spatial resolution of 2° × 2°. For the period of analysis considered here (1978–2009), the SSTs were derived from blended satellite and in situ measurements. In addition, Niño3 and Niño4 indices were obtained from the NOAA's website www.esrl.noaa.gov/psd/data/climateindices/list/.

Following Wang and Fu (2002), the 925-hPa meridional wind spatially averaged over the region 65°W–75°W, 5°S–5°N (Fig. 1a) was used to represent the variability of the cross-equatorial flow over South America (hereafter referred as the South American V-Index), which is an important moisture contributor to feed the Amazon wet season.

In order to identify the role of the global SST warming, ENSO, and AMO modes on the transition length, we computed the three first Rotated Empirical Orthogonal Functions (REOFs) for the global SSTAs in September–October (Schubert et al. 2009). In addition, the role of NASH was explored by considering the mean position of the 1560 m of geopotential height (gpm) line (Li et al. 2011). We performed composite and regression analyses in order to understand the effects of these four modes on the moisture transport and upper-level circulation into South America during the transition season at interannual and decadal scales. Statistical significance of the regressed patterns was determined using an *f* test for the total multiple linear regression, whereas a *t* test was used for the significance of individual regression coefficients. In addition, the statistical significance of correlation coefficients was determined using a *t* test.

3 Results

3.1 Variation of the transition period between the American monsoon systems

Figure 1b shows the corresponding time series of NAM retreat and SAM onset dates expressed in pentads, starting in pentad 45 on August 10 to pentad 70 on December 3. NAM retreat shows a regime shift from late to early retreats after 1990 whereas the southern Amazon wet season shows a significant trend toward late onsets since 1978, as documented by Arias et al. (2012) and Fu et al. (2013), respectively. After removing trends, correlation between both time series is statistically significant during the period considered (−0.37; $P < 0.05$), according to a *t* test. Since autocorrelation in the time series can influence the observed correlation between both variables, the statistical significance of this coefficient was further verified using a random-phase test with 10,000 iterations (Ebisuzaki 1997). This methodology is similar to the bootstrap test, but the random time series created by this method preserves the autocorrelation of the original data instead of its distribution. On the other hand, changes of the NAM onset and the southern Amazon wet season retreat dates are not statistically significant (Fig. 1c), suggesting that the shortening of the American monsoon systems over the last two decades would be mainly due to earlier NAM retreats and delayed southern Amazon wet season onsets.

An earlier NAM retreat and a delayed southern Amazon wet season onset would imply a longer transition period between the American monsoons in boreal fall. Figure 1d shows the length of the transition season between the American monsoon systems, defined as the period between the NAM retreat pentad and the southern Amazon wet season onset pentad (Fig. 1b). The transition between both systems shows a trend toward longer periods, with a linear trend of 1.6 ± 0.6 pentads per decade (i.e. 5.12 ± 1.92 pentads, or 25.6 ± 9.6 days longer between 1978 and 2009). This linear trend and its confidence interval are statistically significant at $P < 0.06$ according to Santer et al. (2000) test. The significance of the linear trend is also supported by the Sen's (1968) test without assuming normal distribution.

Transition seasons were categorized according to their length. Long-transition seasons were defined as those exhibiting lengths larger than the climatological mean length plus 0.8 times the standard deviation (0.8σ) of the transition season length. By contrast, short-transition seasons were defined as those shorter than the climatological mean minus 0.8σ. We identified 7 years with long-transition seasons (1982, 1994, 1995, 1997, 2002, 2004, and 2005), and 10 years with short-transition seasons (1978, 1980, 1981, 1983, 1985, 1986, 1988, 1990, 2006, and 2009). Thus, short-transition seasons were observed mainly before 1990 whereas long-transition seasons occurred mainly after 1990 (Fig. 1d). However, a recovery toward short-transition seasons appears to occur after 2005 in association to later NAM retreats and earlier southern Amazon wet season onsets (Fig. 1b). These results raise the question: what causes the apparent correlation between the changes in the NAM retreat and the southern Amazon wet season onset? As discussed in the introduction, previous studies have identified different factors involved in the recent earlier demise of the NAM and the delayed onsets of the SAM. Particularly, the physical mechanisms for the recent NAM earlier demise have been discussed in Arias et al. (2012). However, how the observed changes in both monsoons are related is not clear. We further explore this question in the next subsections.

3.2 Variations of the cross-equatorial flow over South America

Previous studies have shown that a southerly cross-equatorial flow does not appear to significantly influence the NAM onset since moisture transport to this region is dominated by local low-level jets (Adams and Comrie 1997; Higgins et al. 1997). By contrast, a northerly cross-equatorial flow plays an important role on transporting moisture to the Amazon and the SAM region, eventually triggering monsoon convection (Liebmann et al. 1999; Wang and Fu 2002). Therefore, to identify changes in the cross-equatorial flow over South America during the transition season from NAM to SAM, we compared the composite evolution of the South American V-Index throughout the transition period between the American monsoons for both long and short-transition seasons (Fig. 2). This figure suggests that the northerly flow over South America is weaker during

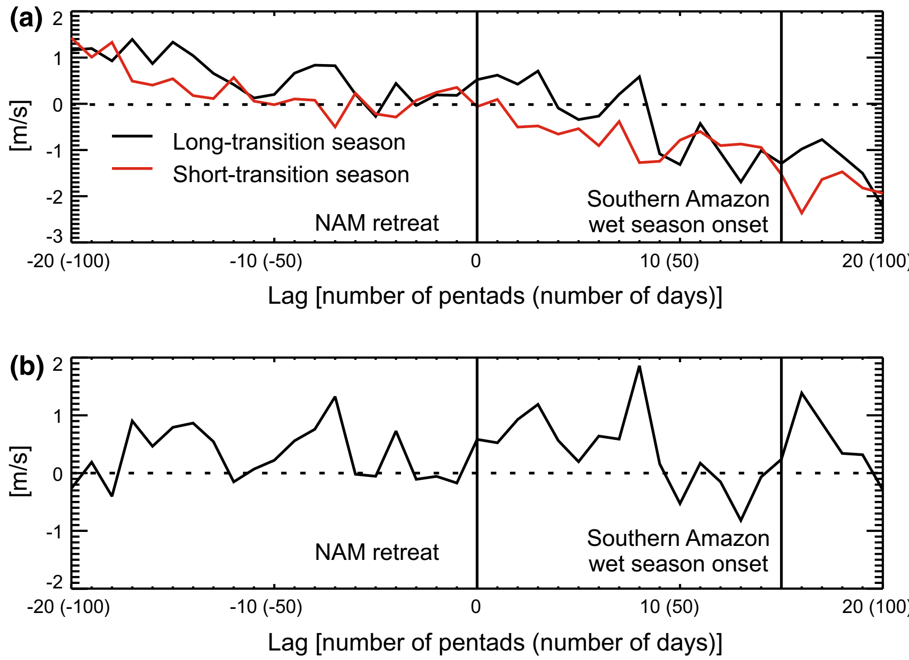

Fig. 2 **a** South American V-Index evolution from NAM to southern Amazon wet season for long (*black*) and short (*red*) transition season years. **b**) South American V-Index difference between long and short-transition seasons. *Solid vertical lines* indicate mean NAM retreat pentad and mean southern Amazon wet season onset pentad during 1978–2009

long-transition season years, as indicated by a less negative V-Index. In contrast, the northerly flow is stronger during the short-transition seasons. Thus, variations of the transition period length between the American monsoons appear to be connected to variations of the cross-equatorial flow over South America.

3.3 Variations of surface and upper-level circulation and associated SSTA changes

3.3.1 Convection and low-level circulation

Figure 2 suggests that long-transition seasons between both monsoon systems are associated with a delayed reversal of the cross-equatorial flow toward the southern Amazon, which would be associated with reduced moisture transport to trigger convection over the Amazon, and therefore, the SAM. To identify the changes of surface circulation and convection during the long-transition seasons with respect to those of the short-transition seasons, Fig. 3a shows the August–September climatology of 850 hPa horizontal wind and GPCP rain rate whereas Fig. 3b shows the composite difference for both variables between long and short-transition seasons. Long-transition seasons are characterized by drier conditions over the SAM domain, the northwestern NAM region, and Central America. By contrast, wetter conditions are observed over the eastern Pacific and western Atlantic Inter-Tropical Convergence Zone (ITCZ), the southern (or tropical) domain of the NAM, and the southeastern (SE) and south central (SC) US. The observed precipitation pattern is consistent with the surface circulation anomalies shown in Fig. 3b. Cyclonic anomalies are observed over the SE and SC US whereas anticyclonic anomalies occur over the northwestern NAM and SAM domains, consistent with enhanced and reduced rainfall over these regions, respectively. In addition, stronger convergence is observed over the eastern Pacific, in agreement with the increased local rainfall amounts, while a southerly surface flow emerges over the northern Amazon, in association with reduced rainfall. The latter is consistent with Fig. 2, which shows an enhanced southerly cross-equatorial flow in South America during the long-transition seasons.

3.3.2 Upper-level circulation

As identified in previous works, large-scale circulations associated with PNA and PSA teleconnection patterns can induce upper-troposphere vorticity anomalies over North and South America, influencing monsoon variability. Figure 3c shows the difference of streamfunction at 0.21-sigma level (i.e., 200 hPa) between long and short-transition seasons in August–September. Both PNA and a PSA-like wave train patterns, extending from the equatorial Pacific to North and South America, respectively, are discernible. Previous studies have shown that PSA-like pattern can induce upper-troposphere anticyclonic (cyclonic) anomalies that in turn increase (reduce) convection over the SAM domain (Liebmann et al. 1999; Grimm et al. 2000). The enhanced subsidence associated with the upper-level anticyclonic anomalous circulation in the SAM domain during the long-transition seasons is consistent with the reduced rainfall observed over the region (Fig. 3b).

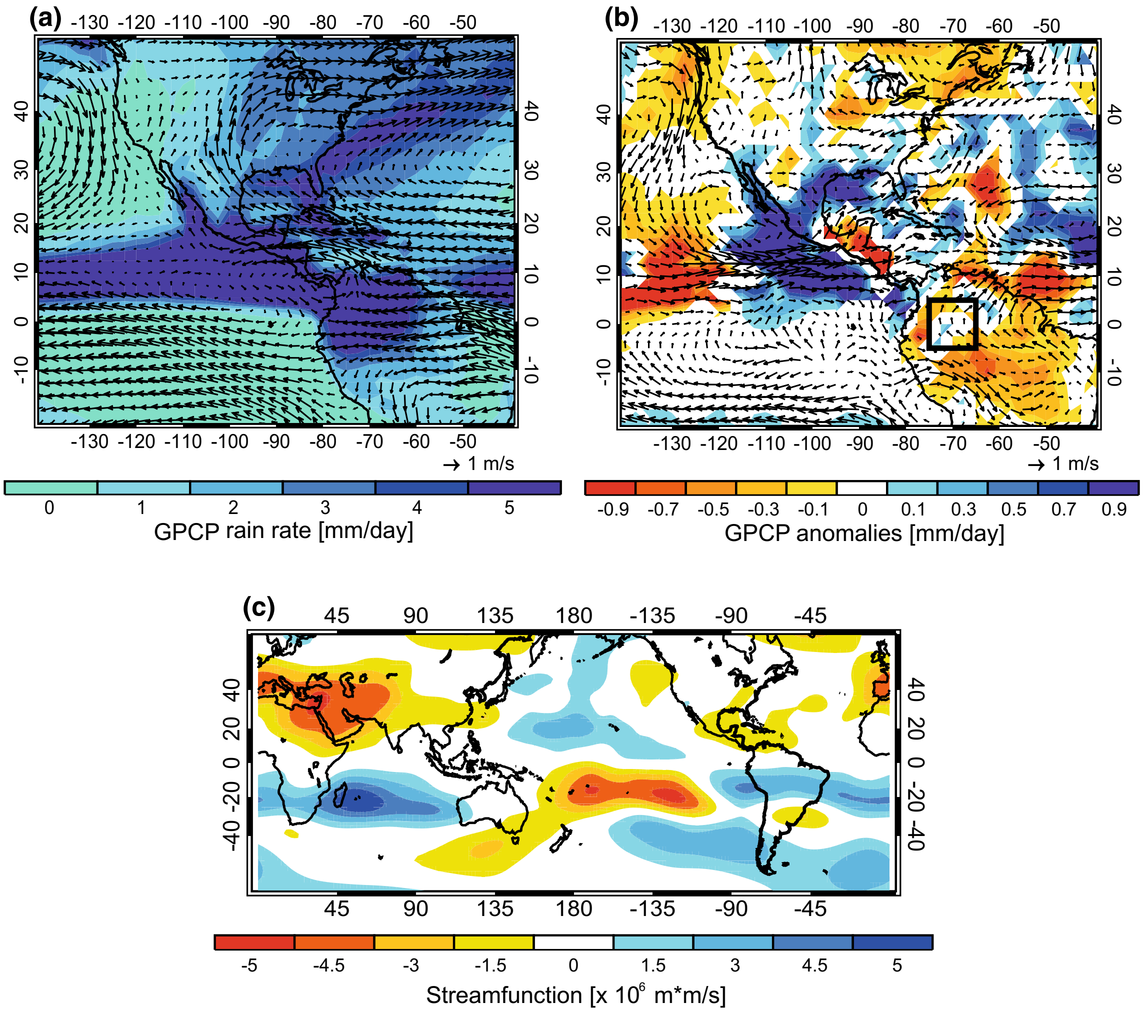

Fig. 3 **a** August–September climatology for 850-hPa zonal wind (*vectors*) and GPCP rain rate anomalies (*shades*). Long-short transition season composite for **b** 850-hPa zonal wind (*vectors*) and GPCP rain rate anomalies (*shades*) and **c** streamfunction at 0.21-sigma level in August–September. In **a** and **b**, the *box* represent the region of the SAM V-Index and the vector scale is shown in the right *bottom* corner of the panel. *Dashed lines* in **c** represent a PSA wave train pattern

3.3.3 Changes of SSTAs

As extensively documented in literature, SSTAs over the global oceans can modulate the American monsoons via direct circulation anomalies and teleconnection patterns. For instance, wave train patterns like the PNA and PSA can be induced by SST changes at different timescales (e.g. Higgins et al. 2000b; Vera et al. 2004; Mo 2000). To characterize the SST changes associated with long and short-transition seasons, the temporal correlation between de-trended time series of transition-season length and SSTAs in August–September was computed (Fig. 4). Statistically significant positive correlations, resembling a Central Pacific Warming (CPW) pattern of El Niño, extend over the tropical central and eastern Pacific, indicating that positive SSTAs in that particular region are related to a lengthening of the transition season. Such warming of the eastern Pacific is consistent with the enhanced ITCZ over the region and the reduced rainfall over Central America observed in Fig. 3b (Schubert et al. 2009). Correlation map for boreal summer (June–September) SSTAs was also computed and has a similar pattern to that in Fig. 4 (not shown). Furthermore, de-trended correlations between transition season length and Niño3 and Niño4 indices are 0.32 and 0.29, respectively (with a statistical significance of 90 and 88 %, respectively). In addition, Fig. 4 also shows statistically significant negative (positive) correlations in the tropical South Atlantic (northeastern Pacific).

How could SSTA over the equatorial Pacific influence the transition season between the American monsoons? Hu et al. (2013) shows a weakening of the interannual variability in the tropical Pacific after 2000, which seems has

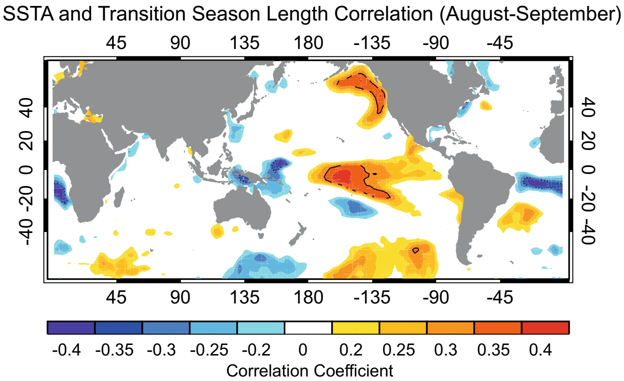

Fig. 4 Correlation coefficient between August–September SSTA and transition season length. Correlation coefficients significant at $P < 0.1$, according to a *t* test, are identified by dotted contours

Fig. 5 Linear regression of 850-hPa winds and GPCP anomalies onto **a** global SST warming mode, **b** ENSO, **c** AMO, and **d** NASH western ridge longitude in August–September–October. **e** Multivariate linear regression onto the four modes. Vector scale is shown on the *bottom right corner* of each panel. The *box* indicates the SAM V-Index region. Only regressed rainfall and winds statistically significant at $P < 0.1$, according to a *t* test (for individual regression coefficients) and an *f* test (for total multiple linear regression), are plotted ▸

altered the frequency and intensity of the more recent El Niño and La Niña events. Moreover, recent studies have shown that the frequency of the CPW events occurred after early 1990's has increased at the expense of the Eastern Pacific Warming (EPW) events (Kim et al. 2009). In addition, several studies have concluded that the impacts of CPW and EPW on different regions are remarkable different (Larkin and Harrison 2005; Ashok et al. 2007; Kim et al. 2009). For instance, PNA/PSA wave trains are enhanced when warm forcing is imposed over the central Pacific (Mo and Paegle 2001; Karoly et al. 1989; Liebmann et al. 2009). Furthermore, the increase of CPW events after mid-1990s has induced an enhancement of wave train patterns in the North Pacific, advecting streamfunction anomalies from the Western North Pacific summer monsoon to the North African and NAM systems (Lee et al. 2014). On the other hand, Ding et al. (2012) show that a marked warming of the central Pacific in boreal summer during the 1980 and the 1990s is associated with enhanced PSA wave train activity. Therefore, the more frequent occurrence of CPW events after the mid-1990s and its associated enhancement of PSA and PNA wave trains coincide with the more frequent occurrence of long-transition seasons between the American monsoons (Fig. 1d) and the associated enhanced PSA/PNA-like activity (Fig. 4). This fact raises a question: could the SST-induced wave train patterns observed since the 1990s, at least partially, contribute to the observed lengthening of the transition season between the American monsoons during the last two decades?

To further clarify this question, we selected CPW years when August-to-October Niño4 index was >1 standard deviation, while Niño3 index stayed below this range (Kim et al. 2009). Likewise, the EPW years were selected when August-to-October Niño3 index was greater than one standard deviation. Thus, 7 CPW (1986, 1991, 1994, 2002, 2004, 2006, and 2009) and 3 EPW (1982, 1987, and 1997) events were selected during 1978–2009. These events agree with those reported in the supplemental material for Kim et al. (2009). Among the 7 long-transition seasons identified between 1978 and 2009, 3 seasons correspond to CPW type of warming (1994, 2002, and 2004), while 2 seasons correspond to EPW (1982 and 1997). Thus, the increase of CPW events since the mid 1990s cannot fully explain the increase of transition season length between the American monsoons. However, the recovery of these monsoons from longer to shorter transition seasons observed after 2005 (Fig. 1d) might be partially related to the recent changes CPW conditions observed in the tropical Pacific (Hu et al. 2013).

The results presented in Figs. 3 and 4 suggest that, on interannual scale, the early demise of the northern NAM and late onset of the Amazon wet season are both associated with El Niño like SSTAs, with intensification of the eastern Pacific and north tropical Atlantic ITCZs, reduced rainfall over Central America, and an enhancement of PNA and PSA wave responses.

3.4 Contributing factors on interannual and decadal scales

The American monsoons are affected by SST variations associated with the global warming trend, ENSO, and AMO. Furthermore, variations in the location of the western ridge of the NASH have been recently documented to be one of the factors associated with the earlier retreats of the NAM observed after the mid-1990s (Arias et al. 2012). Therefore, we evaluated the influence of these four factors on the transition length from the NAM to the SAM. Global SST warming, ENSO, and AMO modes correspond to the first three REOFs of global SSTAs during August–September, respectively (Schubert et al. 2009), whereas the NASH mode is represented by the longitude of its western ridge, as described in Sect. 2. Multivariate regressions of surface winds, rain rate anomalies, and upper-level streamfunction onto these modes were computed. Figure 5 indicates that ENSO and NASH modes (and slightly AMO) partially reproduce the southerly flow over the SAM V-Index region and reduced rainfall over the SAM domain observed during long-transition seasons (Fig. 3b). The global SST warming mode and NASH westward shift can reproduce drier conditions over the northwestern NAM region while the four modes contribute to

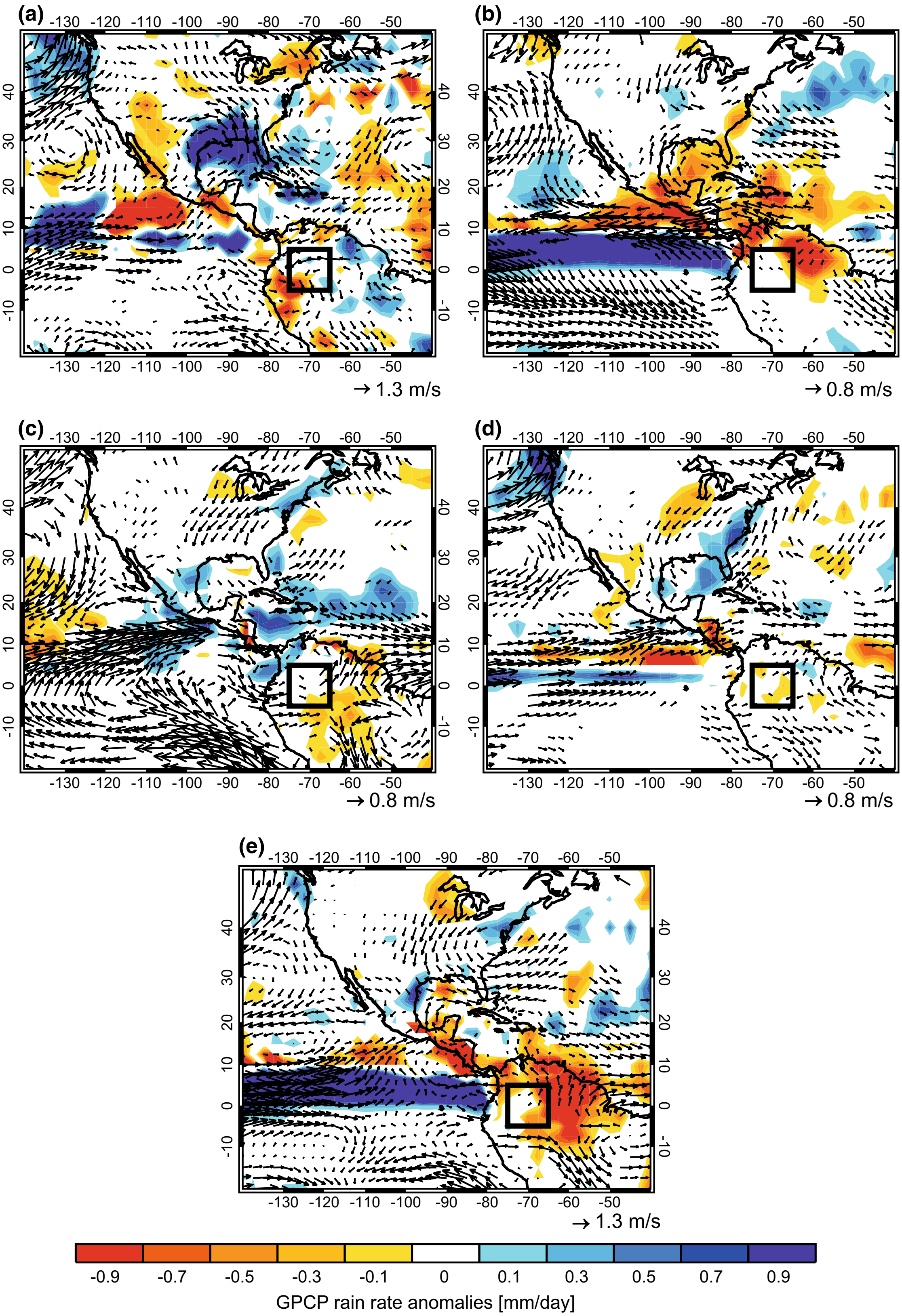
(a)
(b)
(c)
(d)
(e)
-130 -120 -110 -100 -90 -80 -70 -60 -50
-10 0 10 20 30 40
→ 1.3 m/s
→ 0.8 m/s
→ 0.8 m/s
→ 0.8 m/s
→ 1.3 m/s
-0.9 -0.7 -0.5 -0.3 -0.1 0 0.1 0.3 0.5 0.7 0.9
GPCP rain rate anomalies [mm/day]

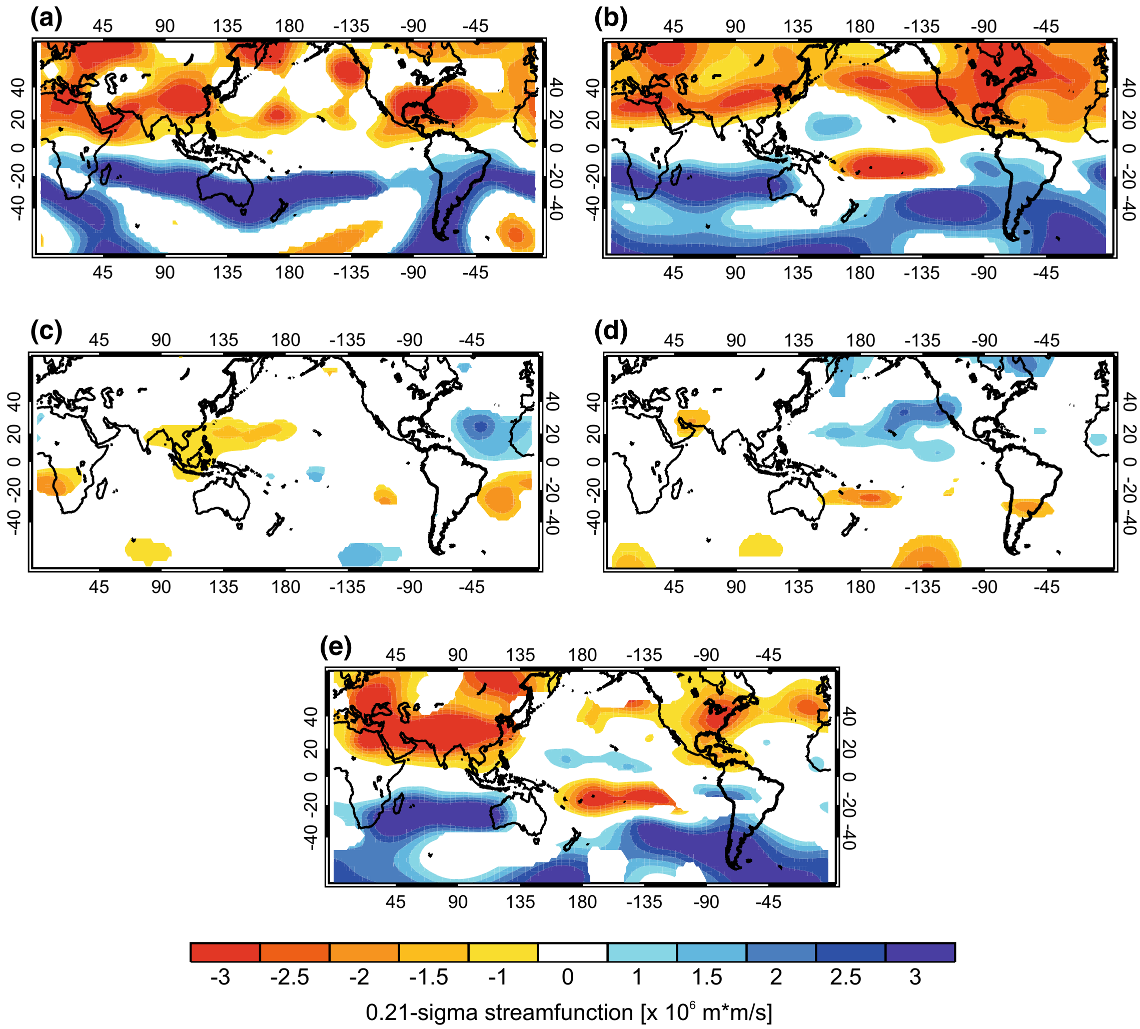

Fig. 6 Linear regression of 0.21-sigma streamfunction onto **a** global SST warming mode, **b** ENSO, **c** AMO, and **d** NASH western ridge longitude in August–September–October. **e** Multivariate linear regression onto the four modes. Only regressed streamfunction statistically significant at $P < 0.1$, according to a t test (for individual regression coefficients) and an f test (for total multiple linear regression), is plotted

drier conditions over the Central American isthmus. Comparing Figs. 5 and 3, it can be observed that the precipitation anomalies in ENSO mode (Fig. 5b) and global SST warming + ENSO + AMO + NASH modes (Fig. 5e) are both located over the east of the SAM V-Index region or northeast of the SAM V-Index region whereas in Fig. 3b, the precipitation anomaly locates the southeast of the V-Index region. Furthermore, the global SST warming and ENSO modes reproduce a PSA pattern, while by contrast, the AMO mode and NASH western ridge composites do not show a clear wave train (Fig. 6).

The contributions identified in Figs. 5 and 6 show the influence of these modes at interannual time-scales. However, whether ENSO is responsible for decadal variability and the observed trends of the NAM retreat and SAM onset needs to be investigated. Thus, we analyzed the regression patterns after removing ENSO influence. ENSO signal was removed by subtracting the linear regression between ENSO mode and the time series corresponding to the variable of interest (precipitation, surface wind, streamfunction) from the variable time series. Since global SST warming and AMO modes are independent from ENSO mode, the ENSO-removed regression patterns for these two modes are not shown. When removing such influence, the total contributions from global SST warming, AMO, and NASH modes reproduce much weaker rainfall reductions over the Central American isthmus and the SAM region and weaker increases of rainfall over the eastern Pacific, indicating that ENSO mode explains such interannual changes (Fig. 7b). However, the increases of rainfall over the southern NAM and Gulf of Mexico are better reproduced when removing these contributions, indicating that these changes

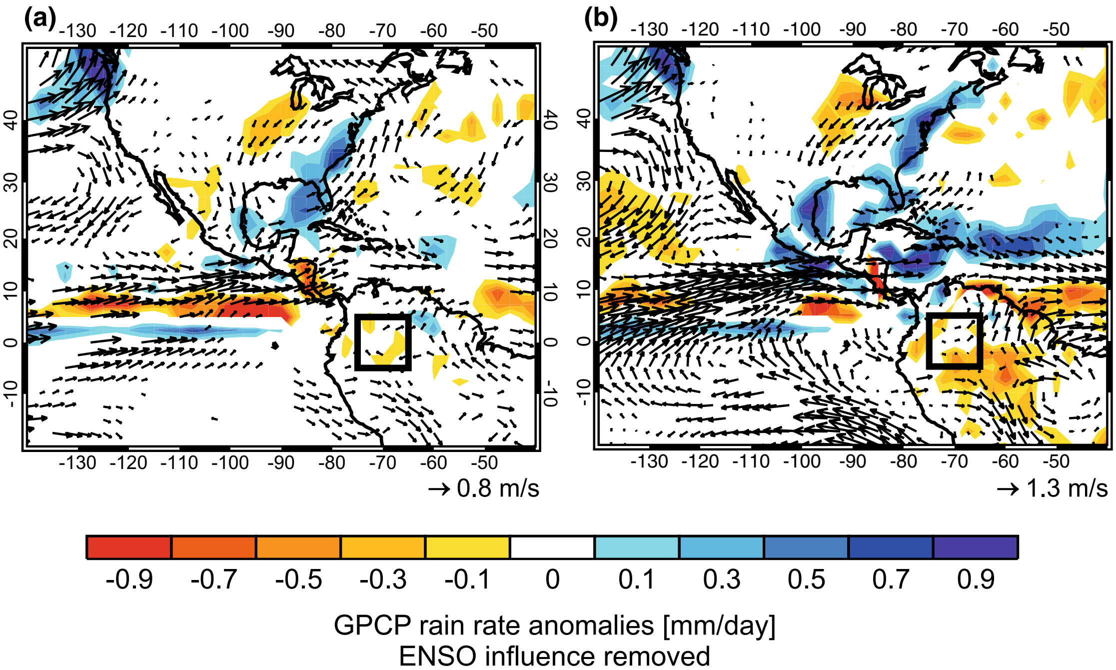

Fig. 7 Same as Fig. 5 but after removing ENSO contributions. **a** NASH western ridge, **b** warming + AMO + NASH modes

occur mainly at decadal scales. A previous study by Wang et al. (2007) indicates that a larger Atlantic warm pool can explain an enhanced western Atlantic ITCZ and associated rainfall over the Gulf of Mexico and the east-central US. Figures 5 and 7 suggest that AMO mode explains the increases of rainfall over the southern NAM whereas global SST warming and NASH modes explain the increased rainfall over the Gulf of Mexico.

In addition, the southerly flow over the SAM V-Index region and the anticyclonic circulation over the northwestern NAM are still observed at decadal scales, mainly in association to the NASH western shift. Respect to the decadal regression patterns of the upper-troposphere streamfunction (Fig. 8), NASH mode shows a similar pattern than that obtained when considering ENSO influence (Fig. 6). When adding the three decadal contributions, a PSA pattern is observed (Fig. 8b), although its trajectory appears to be shifted to the southeast in comparison to that observed in long-transition seasons (Fig. 3c).

The analysis of Figs. 3, 4, 5, 6, 7, 8 suggests that: (1) the enhanced eastern Pacific ITCZ and the reduced convection over the Central American isthmus observed during the long-transition seasons is mainly explained by ENSO at interannual scales, (2) the increased convection over the Caribbean is explained by contributions from global SST warming, AMO, and NASH modes at decadal scales, (3) the increases of rainfall over the southern NAM are mainly associated with AMO whereas the enhanced surface anticyclonic circulation over the northern NAM is associated with AMO and NASH modes at decadal scales, (4) an enhanced southerly SAM V-Index is partially reproduced when considering ENSO and NASH modes (and slightly by AMO, over the eastern SAM V-Index region), and (5) the PSA wave train patterns are explained by contributions from ENSO and global SST warming modes, which appears to occur at both interannual and decadal scales. This suggests that, besides global SST warming, ENSO, and AMO modes, the NASH western ridge location not only contributes to northern NAM earlier retreat but also to SAM delayed onset, mainly on decadal scales, by weakening northerly cross-equatorial flow over South America, which consequently contributes to the delayed monsoon onset observed since 1978.

3.5 Possible mechanisms for the observed lengthening of the transition season

Figure 7 indicates that, after the removal of ENSO, global SST warming, AMO, and NASH modes appear to dry the NAM whereas the global SST warming mode also dries the western SAM region. What are the possible underlying mechanisms for these changes? The stronger and equatorward shifted ITCZ in both northeastern Pacific and north tropical Atlantic suggest a stronger and more equatorward confined rising branch of the regional Hadley cell, which in turn enhances subsidence in the adjacent subtropics, including the NAM and SAM. To further explore this idea, Figs. 9 and 10 show the August–September–October mean

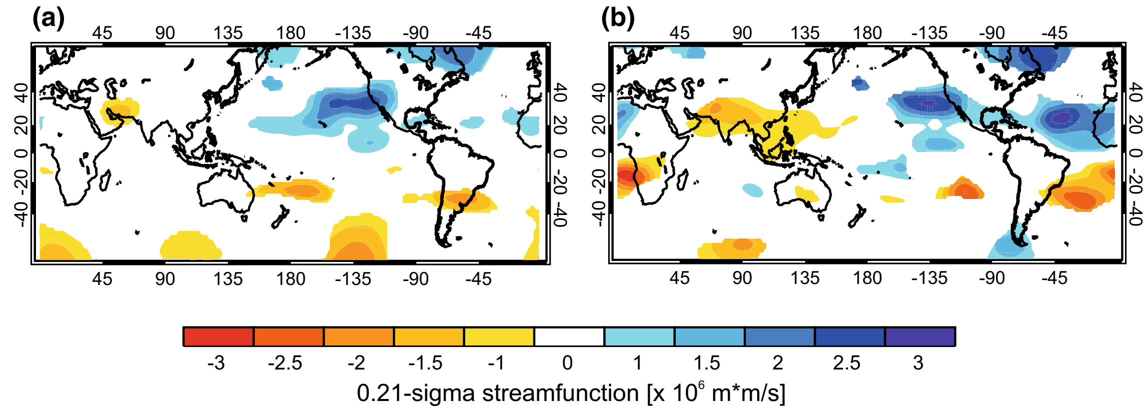

Fig. 8 Same as Fig. 6 but after removing ENSO contributions. **a** NASH western ridge, **b** warming + AMO + NASH modes

vertical cross-sections for the regional meridional divergent circulation and mass streamfunction over North and South America, respectively, during the long and short transition seasons. The boreal summer/fall circulation over both North and South America during long and short-transition seasons occurs in shallow cells (Figs. 9a, b and 10a, b), as documented by Trenberth et al. (2000). When comparing both types of seasons, a stronger regional Hadley cell with rising motion center at 10°N characterizes the long-transition seasons, with enhanced rising motion over the equator and subsidence in the subtropics (Fig. 9c). On the other hand, the regional Hadley cell in South America indicates enhanced subsidence over the northern Amazon and rising motion over the north tropical Atlantic ITCZ during the long-transition seasons compared to short-transition seasons (Fig. 10c), consistently with the precipitation pattern observed in Fig. 3b. Moreover, the zonal divergent circulation over South America indicates enhanced subsidence anomalies over the western Amazon (60°W–40°W) and rising motion over the eastern Pacific (100°W–80°W) during the long-transition seasons (Fig. 11). Therefore, long-transition seasons are associated with an enhanced regional Hadley cell over the Americas and surrounding oceanic ITCZ, enhancing convergence toward the equator and subsidence over the monsoon regions. The regional Walker cells reinforce the local subsidence.

Furthermore, the eastern Pacific ITCZ and southern Mexico are part of the southern domain of the NAM. Therefore, the enhanced convection over these regions shown in Fig. 3b suggests a strengthening or delayed demise of this part of the NAM during the long-transition seasons between both monsoons. Such enhanced convection would also promote surface convergence toward the equator, causing an earlier retreat of the northern NAM and a delayed reversal of the cross-equatorial flow toward South America, which in turn would delay the SAM onset. To explore the latter, Fig. 12 shows the correlation between SAM V-Index and GPCP anomalies in June–July–August (JJA), July–August–September (JAS), and August–September–October (ASO). In order to identify a possible connection beyond the influence of eastern Pacific SSTAs, ENSO influence was removed from both variables by subtracting the variance explained by the Niño3 index from the original variables. Correlations indicate that an anomalous southerly cross-equatorial flow (i.e., positive SAM V-Index anomalies) is associated with (1) enhanced rainfall over the Caribbean Sea and southern NAM region in JJA, JAS, and ASO, (2) reduced rainfall over southern South America in JJA (i.e., its dry season), and (3) reduced rainfall over the northern NAM in JAS and ASO (i.e., its demise phase and transition season toward the SAM). The correlation patterns are very similar when considering ENSO contributions. This appears to suggest that the enhanced convection over the southern NAM during the long-transition seasons observed in Fig. 3b could strengthen a southerly cross-equatorial flow from northern South America to the equator, reducing precipitation over the SAM region during its dry season, which in turn could delay the SAM onset. The analysis of correlations between the August–September GPCP anomalies and leading SAM V-Index anomalies support this result (not shown). This suggests that a stronger or delayed demise of the southern NAM could establish an anomalous southerly regime of the cross-equatorial flow during the transition season, delaying the wet season onset over the southern Amazon.

Moreover, correlations in Fig. 12 indicate that a southerly cross-equatorial flow is associated with reduced rainfall over the Amazon and SAM during the dry season. A stronger dry season over the Amazon is one of the determinant factors involved in the delayed triggering of the wet season over the region (Fu et al. 2013; Yin et al. 2014). Furthermore, Arias et al. (2011) document that increases of the Convective Inhibition Energy over the southern Amazon since 1978 have contributed to reduce convective

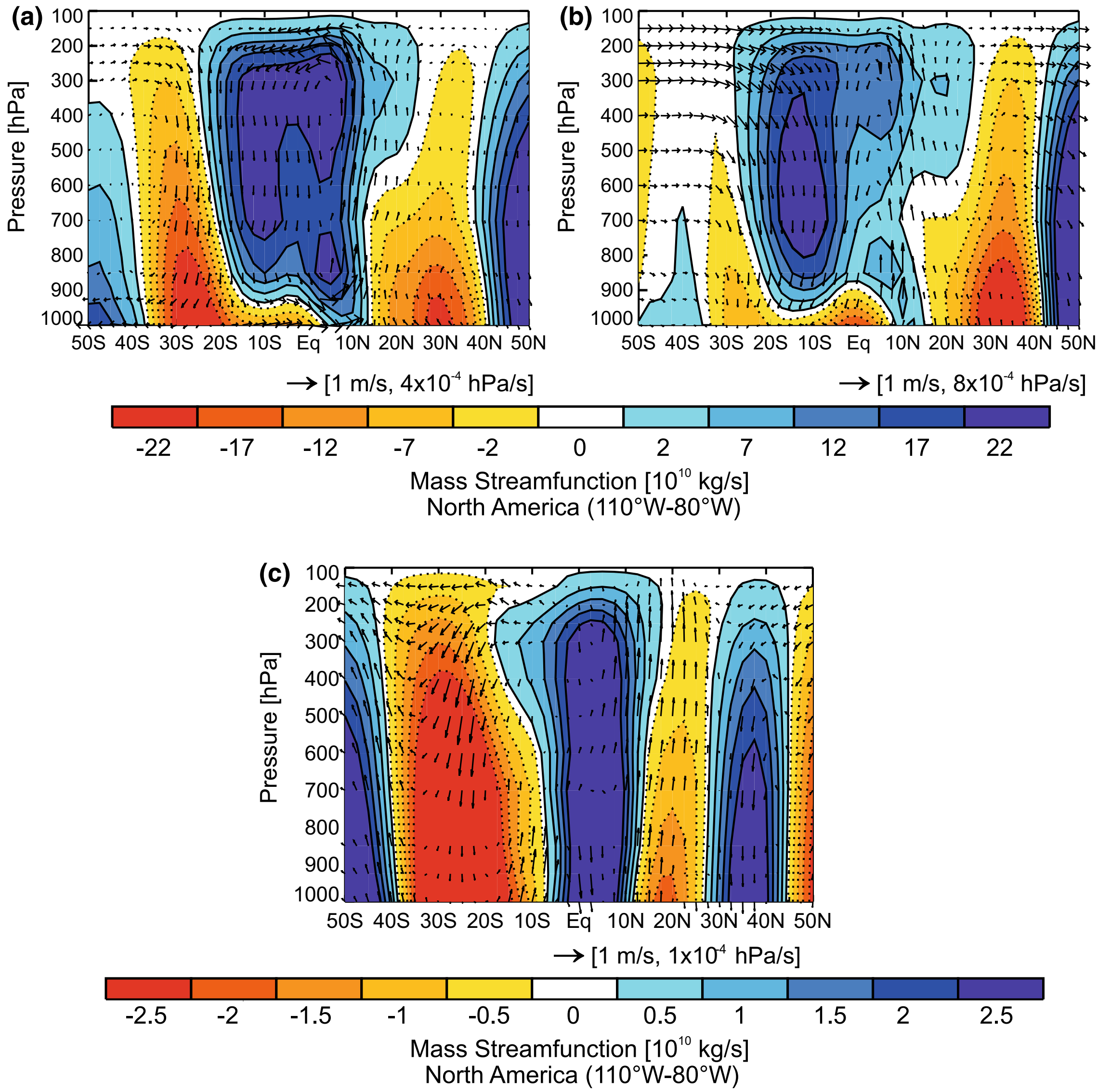

Fig. 9 Vertical cross-sections for regional meridional mass streamfunction (*shades*) and meridional divergent circulation (*vectors*) in August–September–October over North America for **a** long, **b** short, and **c** long-short transition seasons. Vectors are plotted as the divergent meridional wind component and the vertical velocity zonally averaged over the region 110°W–80°W. The vector scale is shown in the *bottom right corner* of each panel

clouds during the transition to the wet season. Therefore, we analyzed the Bowen Ratio anomalies throughout the transition season from NAM to SAM and compared those during long and short-transitions. Figure 13 presents the composite evolution for the difference of Bowen Ratio anomalies between long and short-transition seasons several pentads before and after the NAM retreat. Results indicate that, during the long-transition seasons, surface conditions over SAM and northern NAM are drier several pentads prior the NAM retreat. Conditions over NAM prevail drier even several after its retreat, whereas SAM conditions reduce their dryness around five pentads after the NAM retreats, when SAM onset approaches. This shows that drier land conditions during the long transition seasons lead both NAM retreat and SAM onset, suggesting that the thermodynamic impact of the warming could also contribute to the NAM earlier retreat and SAM delayed onset.

In summary, the stronger and more equatorward regional Hadley cell induced by global SST warming, ENSO, and AMO modes enhances the eastern Pacific and western Atlantic ITCZs as well as the southern NAM, enhancing moisture convergence over the equator. The increased convergence to the equator contributes to an earlier retreat

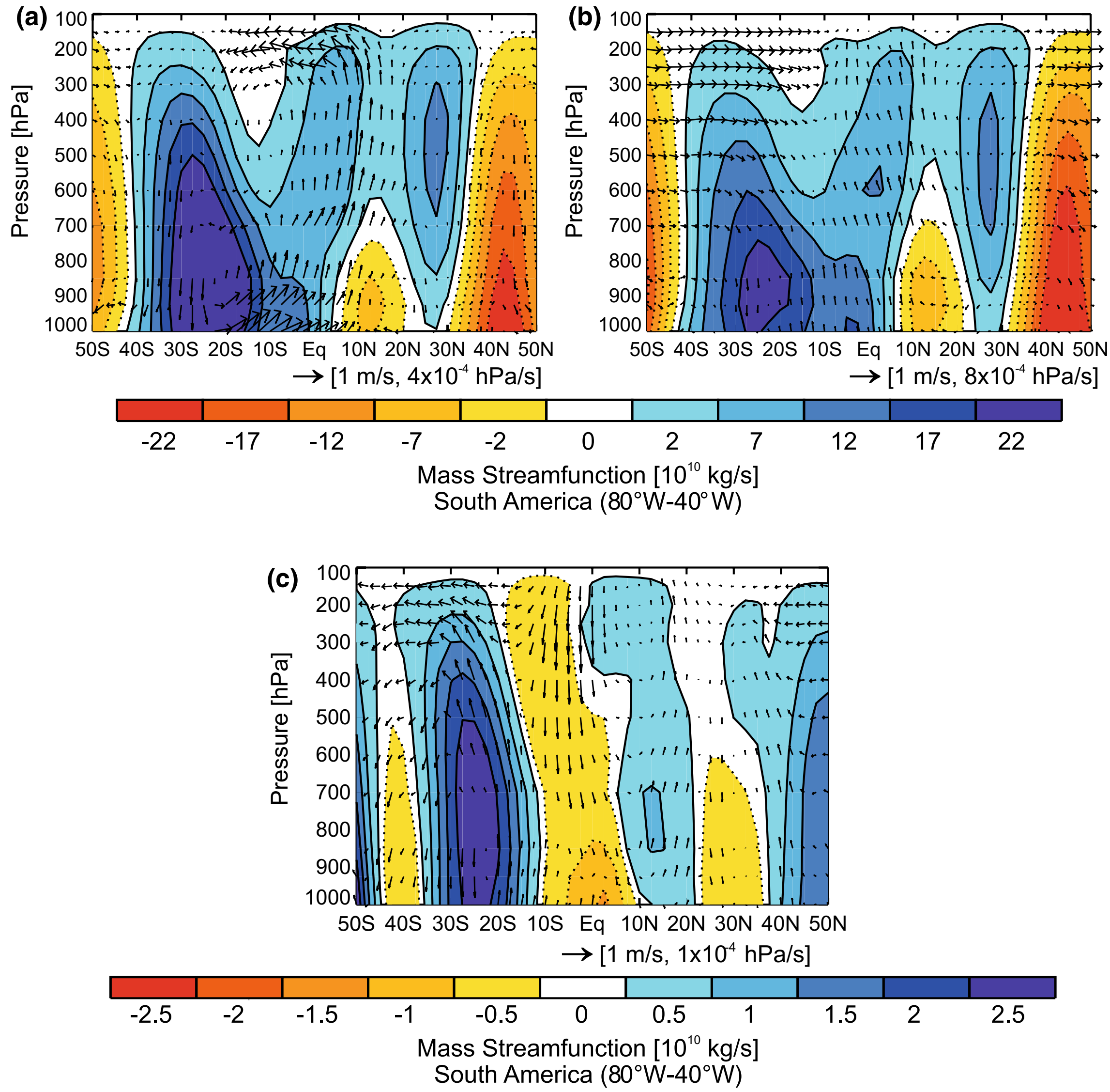

Fig. 10 Same as Fig. 9 but for South America (80°W–40°W)

of the northern NAM and delays the reversal of the cross-equatorial flow toward South America. The latter, in turn delays the wet season onset over the SAM. In addition, the westward shift of the NASH enhances rainfall over the Gulf of Mexico and SC US and contributes to the establishment of southerly anomalies of the cross-equatorial flow in South America, which reinforces the early retreat of the NAM and the delayed onset of the SAM, respectively. Figure 14 presents a scheme for these mechanisms.

Although previous studies have identified the isolated influence of the regional Hadley cell, ENSO, and NASH on the American monsoons, the correlated changes in NAM and SAM through variations of the cross-equatorial flow had not been identified until this study.

4 Discussion

This work identifies a recent correlated shortening of the American monsoon wet seasons and a longer transition between them, in association with earlier NAM retreats since 1990 and a trend toward delayed onsets of the southern Amazon wet season since 1978. The analysis presented here indicates that these changes are partially associated with a westward displacement of the NASH, the global SST warming, ENSO, and AMO modes, and large-scale circulation anomalies resembling the PSA/PNA patterns. Are there another factors contributing to the earlier NAM retreats and late SAM onsets? What could be the root causes of these changes and what are the possible

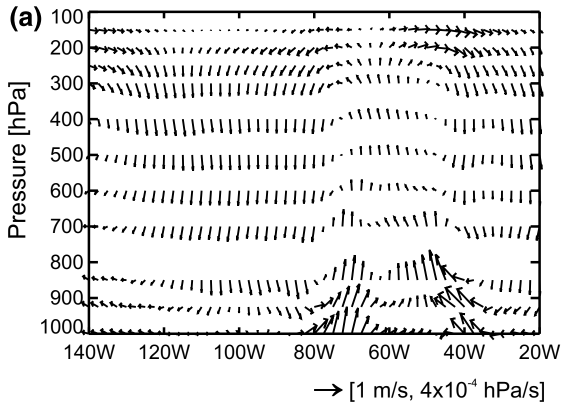

Fig. 11 Vertical cross-sections for regional zonal divergent circulation over South America in August–September–October for **a** long and **b** long-short transition seasons. Vectors are plotted as the divergent meridional wind component and the vertical velocity zonally averaged over 15°S–5°S. The vector scale is shown in the *bottom right corner* of each panel

implications of these results to future changes of the NAM retreat and SAM onset? Although we are not in the position to answer these questions directly in this study, previous studies have suggested the following possibilities:

Kelly and Mapes (2011) indicate that an enhanced Indian monsoon precipitation/Tibetan high strengthens the zonal mean easterlies, which governs the western displacement of the NASH. By contrast, Miyasaki and Nakamura (2005) and Li et al. (2012) suggest that an increase in thermal contrast between the land and ocean (i.e. Africa—Atlantic thermal contrast) may be a more direct forcing for the NASH. While the Indian monsoon influence on NASH would suggest a remote source for the decadal variability of the American monsoons, the land–ocean thermal contrast mechanism would suggest a more regional source for this variability. Therefore, the observed changes in the transition season length between the American monsoons, exerted through NASH variations, could be a consequence of both remote and regional sources of decadal variability.

There are still large uncertainties regarding the changes of the Indian monsoon under an increasing greenhouse gases (GHG) scenario. The weakening of the relationship between ENSO and the Indian monsoon observed after 1976 (Kumar et al. 1999; Krishnamurthy and Goswami 2000; Sarkar et al. 2004) and the compensating influence of the observed shifts in the Walker Circulation and enhanced land-sea contrast (Meehl and Arblaster 2003; Kumar et al. 2006) are some of the uncertainty sources in the projection of this monsoon system under an increased GHG scenario. On the other hand, there is a general consensus among climate models in projecting a GHG concentration increase scenario, a warming pattern of the tropical Pacific, and a stronger land–ocean thermal contrast in summer (e.g. Collins et al. 2010; Yeh et al. 2012; Meehl et al. 2007 and references therein), which in turn would affect the Indian monsoon by different pathways. These uncertainties would in turn induce uncertainties in the projection of future NASH location. However, Li et al. (2012) suggest that the NASH will intensify by the end of the twenty-first century in a GHG concentration increase scenario, predominantly due to an increase in thermal contrast between land and ocean, according to the analysis of Climate Model Intercomparison Project 3 (CMIP3) simulations.

The projections of equatorial Pacific SSTs under an increasing GHG scenario are somehow clearer. Hansen et al. (2006) indicate that, over the past century, warming has been larger in the western equatorial Pacific than in its eastern region, increasing the likelihood of strong El Niño events, whereas other studies have shown that the frequency of CPW events over the equatorial Pacific has been increasing during the last decades (Kim et al. 2009; Lee and McPhaden 2010 and references therein). Yeh et al. (2009) show that future climate projections of anthropogenic climate change using CMIP3 simulations are associated with an increased frequency of CPW events, compared to EPW events, induced by a flattening of the thermocline in the equatorial Pacific. Similar results are found in CMIP5-RCP4.5 simulations (Kim and Yu 2012). On the other hand, several studies have associated the change of the AMO phase in the early 1990s to natural variability and externally forced warming (e.g., Zhang 2007; Ting et al. 2009; Booth et al. 2012). However, Ruiz-Barradas et al. (2014) argue that the CMIP5 models appear to be unable to perturb the regional low-level circulation in the Atlantic, which is a main driver of moisture fluxes, resulting in a poor representation of the spatiotemporal features of the AMO, as well as in the oceanic and hydroclimatic impact associated with the AMO. In addition to ENSO and AMO,

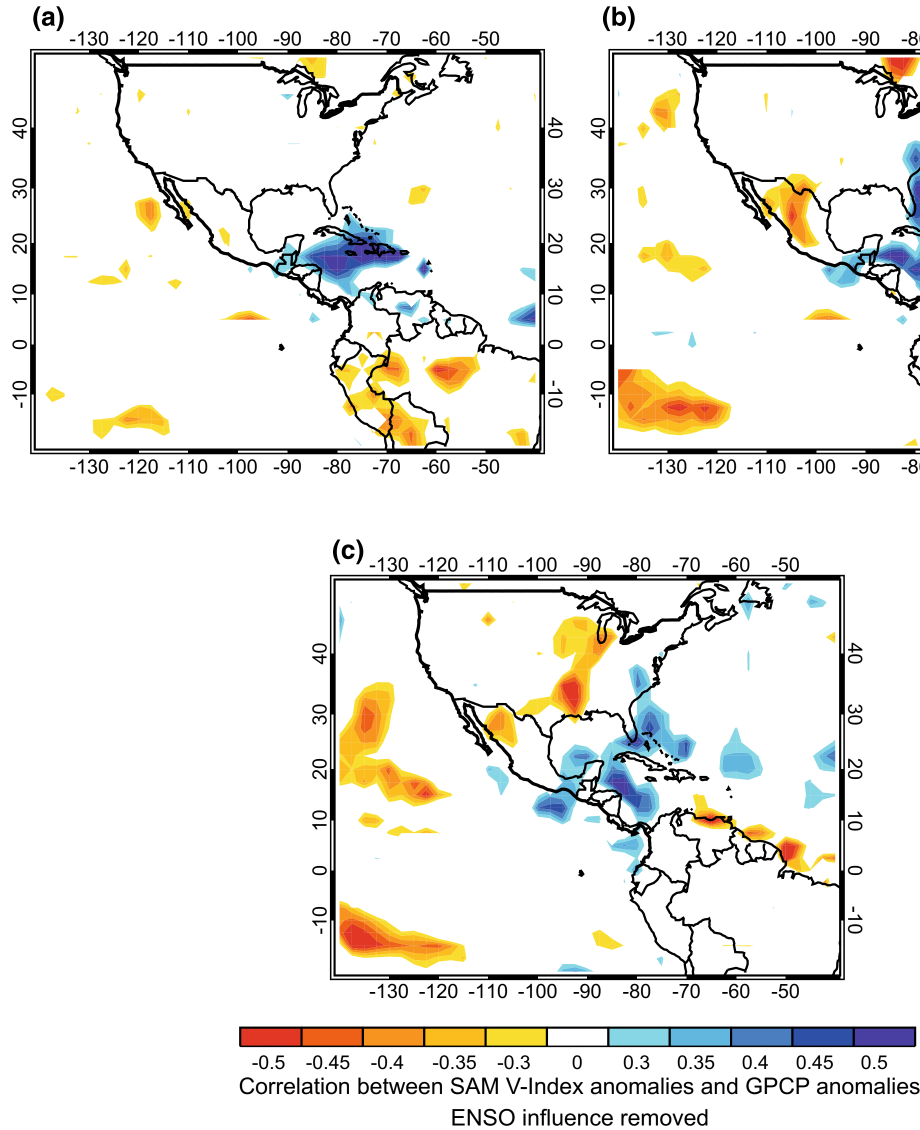

Fig. 12 Correlation between SAM V-Index anomalies and GPCP anomalies for **a** June–July–August, **b** July–August–September, and **c** August–September–October. ENSO influence was previously removed from both variables. Only statistically significant correlations at $P < 0.05$, according to a t test, are plotted

both the NAM retreat and SAM onset changes are found to be associated with the poleward shift of the subtropical jets over both hemispheres in a present and a future climate (Arias et al. 2012; Fu et al. 2013). Such a shift is found to be associated with the broadening of the Hadley cell (Hu et al. 2011; Forster et al. 2011), which could be also forced by the increasing CO2 concentrations in the atmosphere (e.g., Lu et al. 2007).

Other studies have explored the possible influence of a global warming scenario on the American monsoons. For instance, Li et al. (2008) identified a potential anthropogenic influence on Amazon drying during the recent decades using CMIP3 projections. On similar lines, Seth et al. (2010) identified a lengthening of the dry season in the SAM, according to CMIP3 simulations, and hypothesized that this is due to an increased threshold for convection in the warmer, more humid, and stable future climate. A similar result was reported for the global monsoons by Seth et al. (2013) in CMIP5 simulations. In contrast, Jones and Carvahlo (2013) find earlier SAM onset projected in six CMIP5 models. Therefore, conclusions about SAM changes in a future climate seem to depend on the particular metrics used to define monsoon onset, demise, and length, as well as on the specific monsoon region considered (Christensen et al. 2013).

On the other hand, Geil et al. (2014) indicate that the CMIP5 models have improved on representing the NAM

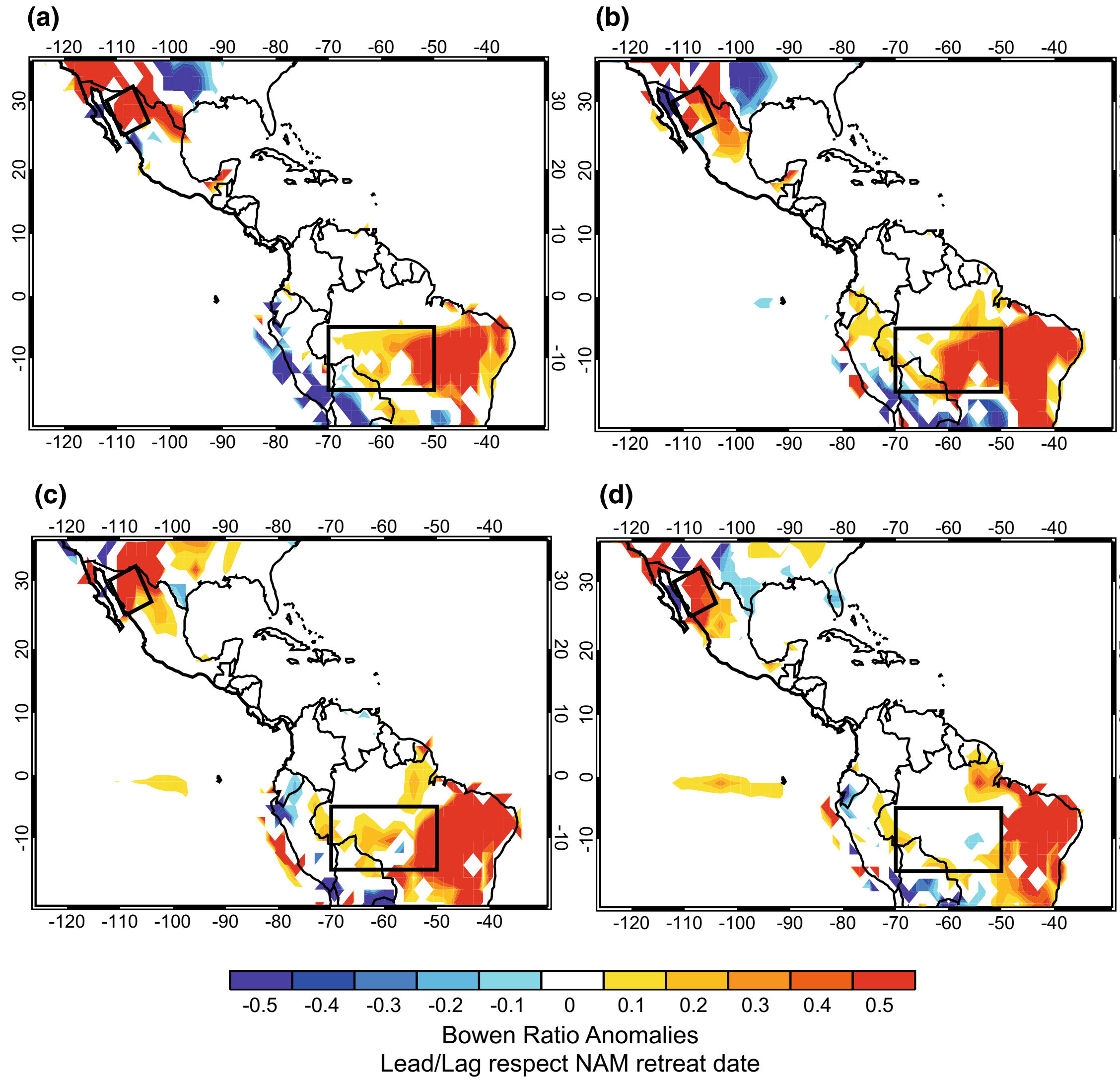

Fig. 13 Lead/lag composite evolution of Bowen ratio difference between long and short-transition seasons throughout the transition season from NAM to SAM. Pentad *zero* indicates the mean NAM retreat date whereas negative (*positive*) pentads correspond to dates before (*after*) NAM retreat date. The *boxes* represent the NAM and SAM domains. **a** Pentad-10, **b** pentad-5, **c** pentad-0, **d** pentad-5

phasing and large-scale circulation patterns at low-levels respect to the CMIP3 generation (Lee et al. 2007; Lin et al. 2008), but still poorly represent monsoon retreat. Cook and Seager (2013) analyzed CMIP5 projections and found that models show significant declines in early monsoon season precipitation due to tropospheric warming and increased instability, whereas precipitation increases in late monsoon season due to the compensating effect of moisture transport during the mature phase of the monsoon, indicating a shift in seasonality toward delayed onsets and demises of the NAM under an increasing GHG scenario.

This discussion then suggests that the shortening of the American monsoons and the lengthening of their transition season observed during the recent decades might be influenced by remote forcing and large-scale changes induced by anthropogenic forcing, which modulate the monsoons at interannual and decadal timescales. Although recent studies have focused on the evaluation of the representation of the American monsoons by the CMIP5 runs and their projections under a global warming scenario, the apparent contradictory results on future SAM projections and the possible changes of the NAM throughout its different stages need to be addressed by testing the possible mechanisms proposed in this study with the CMIP5 simulations. Furthermore, the role of vegetation and land use in modulating or driving these observed changes needs to be also addressed.

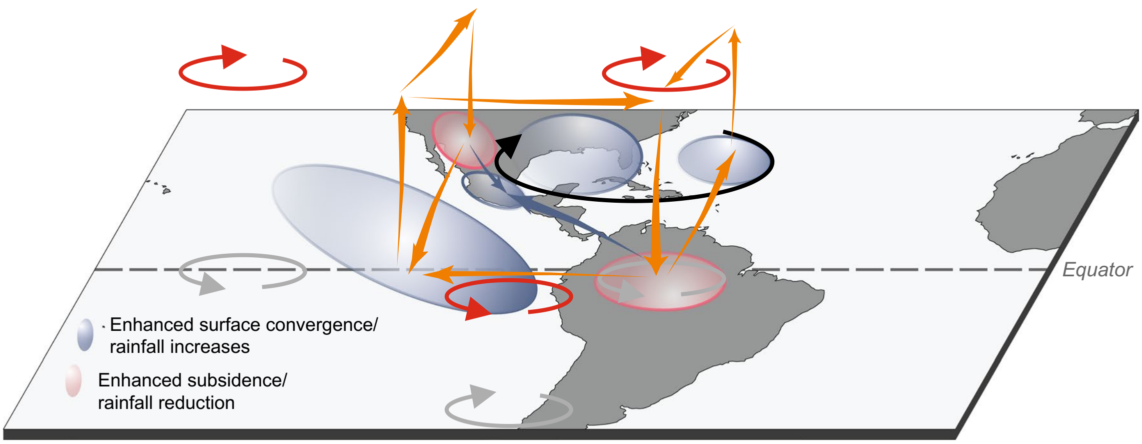

Fig. 14 Scheme of the mechanisms and modulators involved in the recent shortening of the American monsoons. During long-transition seasons from NAM to SAM, the regional Hadley and Walker cells (*orange arrows*) strengthen, inducing convergence over the Intra-American region and the eastern Pacific (*light blue shades*). This convergence strengthens the cross-equatorial flow in both hemispheres toward the equator (*blue arrows*), reducing rainfall over the American monsoon domains (*light red shades*). The main modulators of these mechanisms are the global SST warming, ENSO, and AMO modes. Particularly, the ENSO mode is related to an enhanced PSA pattern, represented by upper troposphere cyclones/anticyclones (*red*) and their surface counterpart anticyclones/cyclones (*grey*) in the Southern Hemisphere. In addition, a fourth element associated with these changes is the westward shift of the NASH (*black* anticyclone in the Northern Hemisphere), which reduces moisture transport to the NAM and is related to a northward cross-equatorial flow over South America

5 Summary

An analysis of the dynamical conditions explaining the correlated shorter monsoon seasons in the Americas and a longer transition season between these systems during the period 1978–2009 is presented here. Results suggest that such changes are associated with a regime shift toward earlier retreats of the NAM and delayed onsets of the southern Amazon wet season. In particular, the longest transition seasons are observed after the earlier retreats of the NAM. Our results show that the observed lengthening of the transition season between both systems is associated with global SST warming, ENSO, and AMO modes, and the strengthening of PNA/PSA wave train patterns, and a westward shift of the NASH.

Our analysis of surface circulation, upper-level streamfunction, precipitation anomalies and SSTAs indicate that the lengthening of the transition season from NAM to SAM is associated with a stronger and more equatorward regional Hadley cell induced by global SST warming, ENSO, and AMO modes, which strengthens the eastern Pacific and western Atlantic ITCZs as well as the southern NAM, enhancing moisture convergence over the equator. Such increased convergence to the equator contributes to an earlier retreat of the northern NAM and delays the reversal of the cross-equatorial toward South America. The latter, in turn delays the wet season onset over the SAM due to a reduction of moisture transport toward the region. In addition, a westward shift of the NASH enhances rainfall over the Gulf of Mexico and SC US and contributes to the establishment of southerly anomalies of the cross-equatorial flow in South America, which reinforces the early retreat of the NAM and the delayed onset of the SAM, respectively. Furthermore, our results appear to suggest that the thermodynamic response to warming could induce drier land conditions over both monsoon regions during the late boreal summer, contributing to an earlier demise of the NAM and strengthening the SAM dry season, which in turn could influence the wet season onset over this region. However, further research on how local land conditions are related to the observed changes in the American monsoons need to be addressed.

Finally, we speculate that the recent correlated shortening of the American monsoon systems, driven by large-scale circulation changes observed since 1978, might be partially a consequence of the increasing GHG concentration in the atmosphere, based on available evidence. Such possible connection highlights the need to further investigate the root causes of the shortening of the NAM and SAM in a changing climate. Especially, the causes of the changes of the NASH, the enhanced PSA/PNA-like patterns, and the global SST warming, ENSO, and AMO modes need to be further explored in order to improve our understanding, prognostic, and projection of the American monsoon systems.

Acknowledgments PA was supported by "Comisión Nacional de Investigación Científica y Tecnológica de Chile" grant FONDECYT #3140570 and Program "Estrategia de Sostenibilidad 2014–2015" at Universidad de Antioquia. RF was supported by the National Science Foundation grant (AGS-0937400) and the NOAA Climate Program

Office Climate Prediction Program for the Americas (CPPA) Grant (NA10OAR4310157). CV acknowledges support from CONICET/PIP 112-20120100626CO and UBACyT 20020130100489BA. MR acknowledges support from FONDAP-CONICYT n. 15110009 and NC120066. PA and MR are part of the Center for Climate and Resilience Research (CR2), Center of Excellence FONDAP-CONICYT n. 15110009, Chile. We acknowledge the insightful comments from two anonymous reviewers and the editor. Finally, we thank Vincent Combes for his help with Fig. 14.

References

Adams DK, Comrie AC (1997) The North American monsoon. Bull Am Meteorol Soc 78:2197–2213

Adler RF, Huffman GJ, Chang A, Ferraro R, Xie P, Janowiak J, Rudolf B, Schneider U, Curtis S, Bolvin D, Gruber A, Suskind J, Arkin P (2003) The version 2 global precipitation climatology project (GPCP) monthly precipitation analysis (1979-present). J Hydrometeorol 4:1147–1167

Anderson BT, Kanamaru H, Roads JO (2004) The summertime atmospheric hydrologic cycle over the southwestern United States. J Clim 5:679–692

Apaestegui J, Cruz FW, Siffedine A, Espinoza JC, Guyot JL, Khodri M, Strikis N, Santos RV, Cheng H, Edwards L, Carvalho E, Santini W (2014) Hydroclimate variability of the South American monsoon system during the last 1600 years inferred from speleothem isotope records of the north-eastern Andes foothills in Peru. Clim Past Discuss 10:533–561

Arias PA, Fu R, Hoyos CD, Li W, Zhou L (2011) Decadal changes in cloudiness over the Amazon forests: observations and potential causes. Clim Dyn 37(5):1151–1164. doi:10.1007/s00382-010-0903-2

Arias PA, Fu R, Mo K (2012) Changes in monsoon regime over northwestern Mexico in recent decades and its potential causes. J Clim 25:4258–4274

Ashok K, Behera SK, Rao SA, Weng H, Yamagata T (2007) El Niño Modoki and its possible teleconnection. J Geophys Res 112:C11007. doi:10.1029/2006JC003798

Barlow M, Nigam S, Berbery EH (1998) Evolution of the North American monsoon system. J Clim 11:2238–2257

Berbery EH, Barros VR (2002) The hydrologic cycle of the La Plata basin in South America. J Hydrometeorol 3:630–645

Booth BB, Dunstone NJ, Halloran PR, Andrews T, Bellouin N (2012) Aerosols implicated as a prime driver of the twentieth-century North Atlantic climate variability. Nature 484:228–232

Castro CL, McKee TB, Pielke RA Sr (2001) The relationship of the North American monsoon to tropical and North Pacific Sea surface temperatures as revealed by observational analyses. J Clim 14:4449–4473

Castro CL, Pielke RA, Adegoke JO, Schubert SD, Pegion PJ (2007) Investigation of the summer climate of the contiguous United States and Mexico using the regional atmospheric modeling system (RAMS). Part II: model climate variability. J Clim 20:3866–3887

Chiessi CM, Mulitza S, Patzold J, Wefer G, Marengo JA (2009) Possible impact of the Atlantic multidecadal oscillation on the South American summer monsoon. Geophys Res Lett 36:L21707. doi:10.1029/2009GL039914

Christensen JH, Krishna Kumar K, Aldrian E, An S-I, Cavalcanti IFA, de Castro M, Dong W, Goswami P, Hall A, Kanyanga JK, Kitoh A, Kossin J, Lau N-C, Renwick J, Stephenson DB, Xie S-P, Zhou T, Zhou T (2013) Climate phenomena and their relevance for future regional climate change. In: Stocker TF, Qin D, Plattner G-K, Tignor M, Allen SK, Boschung J, Nauels A, Xia Y, Bex V, Midgley PM (eds) Climate change 2013: the physical science basis. Contribution of working group I to the fifth assessment report of the intergovernmental panel on climate change. Cambridge University Press, Cambridge

Collins M et al (2010) The impact of global warming on the tropical Pacific Ocean and El Niño. Nat Geosci 3(6):391–397. doi:10.1038/ngeo868

Cook BI, Seager R (2013) The response of the North American monsoon to increased greenhouse gas forcing. J Geophys Res Atmos 118:1690–1699. doi:10.1002/jgrd.50111

da Silva GAM, Drumond A, Ambrizzi T (2011) The impact of El Niño on South American summer climate during different phases of the Pacific decadal oscillation. Theor Appl Climatol 106:307–319

Ding Q, Steig EJ, Battisti DS, Wallace JM (2012) Influence of the tropics on the Southern annular mode. J Clim 25:6330–6348

Douglas AV, Englehart P (2007) A climatological perspective of transient synoptic features during NAME 2004. J Clim 20:1947–1954

Douglas MW, Maddox RA, Howard K, Reyes S (1993) The Mexican monsoon. J Clim 6:1665–1677

Ebisuzaki W (1997) A method to estimate the statistical significance of a correlation when the data are serially correlated. J Clim 10:2147–2153

Enfield DB, Mestas-Nuñez AM, Trimble PJ (2001) The atlantic multidecadal oscillation and its relationship to rainfall and river flows in the continental U.S. Geophys Res Lett 28:2077–2080

Figueroa SN, Nobre C (1990) Precipitation distribution over central and western tropical South America. Climanalise 5:36–44

Figueroa SN, Satyamurty P, Silva Dias PLD (1995) Simulations of the summer circulation over the South American region with an Eta coordinate Model. J Atmos Sci 52:1573–1584

Forster PM et al. (2011) Stratospheric changes and climate. Scientific assessment of ozone depletion: 2010. Global Ozone research and monitoring project—report no. 52. World meteorological organization, Geneva, Switzerland, 1-60

Fu R, Yin L, Li W, Arias PA, Dickinson RE, Huang L, Chakraborty S, Fernandes K, Liebmann B, Fisher R, Myneni R (2013) The increase of dry season length over the southern Amazonia in recent decades and its implications for climate projection. Proceed. Natl. Acad. Sci. doi:10.1073/pnas.1302584110

Fu R, Arias PA, Wang H (2014) Connection between the North and South American monsoons. In: The monsoons and climate change. Eds. Leila M.V. Carvalho and Charles Jones. Springer Link, in press

Geil KL, Serra YL, Zeng X (2014) Assessment of CMIP5 model simulations of the North American monsoon system. J Clim 26:8887–8901

Giannini A, Chiang JCH, Cane M, Kushnir Y, Seager R (2001) The ENSO teleconnection to the tropical Atlantic Ocean: contributions of the remote and local SSTs to rainfall variability in the tropical Americas. J Clim 14:4530–4544

Gonzalez M, Vera C, Liebmann B, Marengo J, Kousky V, Allur D (2007) The nature of the rainfall onset over central South America. Atmósfera 20(4):379–396

Grimm AM (2011) Interannual climate variability in South America: impacts on seasonal precipitation, extreme events and possible effects of climate change. Stoch Environ Res Risk A 25:537–554. doi:10.1007/s00477-010-0420-1

Grimm AM, Ferraz S, Gomez J (1998) Precipitation anomalies in southern Brazil associated with El Niño and La Niña events. J Clim 11:2863–2880

Grimm AM, Barros VR, Doyle ME (2000) Climate variability in southern South America associated with El Niño and La Niña events. J Clim 13:35–58

Hansen J, Sato M, Ruedy R, Lo K, Lea D, Medina-Elizade M (2006) Global temperature change. Proceed Natl Acad Sci 103(39):14288–14293
Higgins RW, Shi W (2000) Dominant factors responsible for interannual variability of the summer monsoon in the southwestern United States. J Clim 13:759–776
Higgins RW, Janowiak JE, Wang X (1997) Influence of the North American monsoon system on the United States summer precipitation regime. J Clim 10:2600–2622
Higgins RW, Mo KC, Yao Y (1998) Interannual variability of the U.S. summer precipitation regime with emphasis on the southwestern monsoon. J Clim 11:2582–2606
Higgins RW, Chen Y, Douglas AV (1999) Interannual variability of the North American warm season precipitation regime. J Clim 12:653–680
Higgins RW, Shi W, Yarosh E, Joyce R (2000a) Improved United States precipitation quality control system and analysis NCEP/Climate Prediction Center ATLAS No.7, NCEP/NWS/NOAA, 40 pp
Higgins RW, Leetmaa A, Xue Y, Barnston A (2000b) Dominant factors influencing the seasonal predictability of U.S. precipitation and surface air temperature. J Clim 13:3994–4017
Hu Q, Feng S (2008) Variation of the North American summer monsoon regimes and the Atlantic multidecadal oscillation. J Clim 21(11):2371–2383
Hu Q, Feng S (2010) Influence of the Arctic oscillation on central United States summer rainfall. J Geophys Res 115:D01102. doi:10.1029/2009JD011805
Hu YY, Zhou C, Liu JP (2011) Observational evidence for the poleward expansion of the Hadley circulation. Adv Atmos Sci 28:33–44
Hu Z-Z, Kumar A, Ren HL, Wang H, L'Heureux M, Jin F-F (2013) Weakened interannual variability in the tropical Pacific Ocean since 2000. J Clim 26(8):2601–2613
Jones C, Carvalho LMV (2013) Climate change in the South American monsoon system: present climate and CMIP5 projections. J Clim 26:6660–6678
Kalnay E, Kanamitsu M, Kistler R, Collins W, Deaven D, Gandin L, Iredell M, Saha S, White G, Woollen J, Zhu Y, Chelliah M, Ebisuzaki W, Higgins W, Janowiak J, Mo K, Ropelewski C, Wang J, Leetma A, Reynolds R, Jenne R, Joseph D (1996) The NCEP-NCAR 40-year reanalysis project. Bull Am Meteorol Soc 77:437–471
Karoly D, Plumb RA, Ting M (1989) Examples of the horizontal propagation of quasi-stationary waves. J Atmos Sci 46:2802–2811
Kelly P, Mapes BE (2011) Zonal mean wind, the Indian monsoon, and July drying in the western Atlantic subtropics. J Geophys Res 116:D00Q07. doi:10.1029/2010JD015405
Kim ST, Yu J-Y (2012) The two types of ENSO in CMIP5 models. Geophys Res Lett 39:L11704. doi:10.1029/2012GL052006
Kim HM, Webster PJ, Curry JA (2009) Impact of shifting patterns of pacific ocean warming on north atlantic tropical cyclones. Science 325(5936):77–80
Krishnamurthy V, Goswami BN (2000) Indian monsoon-ENSO relationship on interdecadal timescale. J Clim 13:579–595
Kumar K, Rajagopalan B, Cane MA (1999) On the weakening relationship between the Indian monsoon and ENSO. Science 284:2156–2159
Kumar K, Rajagopalan B, Hoerling M, Bates G, Cane M (2006) Unraveling the mystery of Indian monsoon failure during El Niño. Science 314:115
Kushnir Y, Seager R, Ting M, Naik N, Nakamura J (2010) Mechanisms of tropical atlantic SST influence on North American hydroclimate variability. J Clim 23:5610–5628
Larkin NK, Harrison DE (2005) Global seasonal temperature and precipitation anomalies during El Niño autumn and winter. Geophys Res Lett 32:L13705. doi:10.1029/2005GL022738
Lee T, McPhaden MJ (2010) Increasing intensity of El Niño in the central-equatorial Pacific. Geophys Res Lett 37:L14603. doi:10.1029/2010GL044007
Lee M-I et al (2007) Sensitivity to horizontal resolution in the AGCM simulations of warm season diurnal cycle of precipitation over the United States and northern Mexico. J Clim 20:1862–1881
Lee EJ, Ha K-J, Jhun J-G (2014) Interdecadal changes in interannual variability of the global monsoon precipitation and interrelationships among its subcomponents. Clim Dyn 42:2585–2601. doi:10.1007/s00382-013-1762-4
Lenters JL, Cook KH (1996) Simulation and diagnosis of the regional South American precipitation climatology. J Clim 8:2988–3005
Li W, Fu R (2004) Transition of the large-scale atmospheric and land surface conditions from the dry to the wet season over Amazonia as diagnosed by the ECMWF reanalysis. J Clim 17:2637–2651
Li W, Fu R (2006) Influence of cold air intrusions on the wet season onset over Amazonia. J Clim 19:257–275
Li W, Fu R, Negron-Juarez R, Fernandes K (2008) Observed change of the standardized precipitation index, its potential cause and implications to future climate change in the Amazon region. Proceed R Soc Lond Biol Sci 363(1498):1767–1772
Li W, Li L, Fu R, Deng Y, Wang H (2011) Changes to the north atlantic subtropical high and its role in the intensification of summer rainfall variability in the southeastern United States. J Clim 24:1499–1506
Li W, Li L, Ting M, Liu Y (2012) Intensification of Northern Hemisphere subtropical highs in a warming climate. Nat Geosci 5:830–834
Liebmann B, Allured D (2005) Daily precipitation grids for South America. Bull Am Meteorol Soc 86:1567–1570
Liebmann B, Kiladis GN, Marengo JA, Ambrizzi T, Glick JD (1999) Submonthly convective variability over South America and the South Atlantic convergence zone. J Clim 12:1877–1891
Liebmann B, Kiladis GN, Carvalho LMV, Jones C, Vera CS, Bladé I, Allured D (2009) Origin of convectively coupled kelvin waves over south America. J Clim 22:300–315
Lin JL, Mapes BE, Weickmann KM, Kiladis GN, Schubert SD, Suarez MJ, Bacmeister JT, Lee MI (2008) North American monsoon and convectively coupled equatorial waves simulated by IPCC AR4 coupled GCMs. J Clim 21:2919–2937
Lu J, Vecchi GA, Reichler T (2007) Expansion of the Hadley cell under global warming. Geophys Res Lett 34:L06805. doi:10.1029/2006GL028443
Marengo JA, Soares W, Saulo W, Nicolini M (2004) Climatology of the LLJ east of the Andes as derived from the NCEP reanalyses. J Clim 17:2261–2280
Marengo JA, Liebmann B, Grimm AM, Misra V, Silva Dias PL, Cavalcanti IFA, Carvalho LMV, Berbery EH, Ambrizzi T, Vera CS, Saulo AC, Nogués-Paegle J, Zipser E, Seth A, Alves LM (2010) Recent developments on the South American monsoon system. Int J Climatol 32(1):1–21. doi:10.1002/joc2254
McCabe GJ, Palecki MA, Betancourt JL (2004) Pacific and Atlantic Ocean influences on multidecadal drought frequency in the United States. Proceed Natl Acad Sci. 101:4136–4141
Mechoso CR, Lyons S, Spahr J (1990) The impact of sea surface temperature anomalies on the rainfall in northeast Brazil. J Clim 3:812–826
Meehl GA, Arblaster JM (2003) Mechanisms for projected future changes in south Asian monsoon precipitation. Clim Dyn 21:659–675
Meehl GA, Stocker TF, Collins WD, Friedlingstein P, Gaye AT, Gregory JM, Kitoh A, Knutti R, Murphy JM, Noda A, Raper SCB, Watterson IG, Weaver AJ, Zhao Z-C (2007) Global climate projections. In: Solomon S, Qin D, Manning M, Chen Z, Marquis M, Averyt KB, Tignor M, Miller HL (eds) Climate change

2007: the physical science basis. Contribution of working group I to the fourth assessment report of the intergovernmental panel on climate change. Cambridge University Press, Cambridge
Miyasaka T, Nakamura H (2005) Structure and formation mechanisms of the Northern hemisphere summertime subtropical highs. J Clim 18:5046–5065
Mo KC (2000) Relationships between low-frequency variability in the Southern Hemisphere and sea surface temperature anomalies. J Clim 13:3599–3610
Mo KC (2010) Interdecadal modulation of the impact of ENSO on precipitation and temperature over the United States. J Clim 23(13):3639–3656
Mo KC, Nogues-Paegle J (2001) The Pacific South American modes and their downstream effects. Int J Climatol 21:1211–1229
Moura AD, Shukla EJ (1981) On the dynamics of the droughts in northeast Brazil: observations, theory and numerical experiments with a general circulation model. J Atmos Sci 38:2653–2673
Munoz E, Wang C, Enfield D (2010) The intra-americas springtime sea surface temperature anomaly dipole as fingerprint of remote influences. J Clim 23:43–56
Paegle JN, Mo KC (2002) Linkages between summer rainfall variability over South America and sea surface temperature anomalies. J Clim 15:1389–1407
Pisciottano G, Diaz A, Cazes G, Mechoso CR (1994) El Niño-Southern oscillation impact on rainfall in uruguay. J Clim 7:1286–1302
Raia A, Cavalcanti IFA (2008) The life cycle of the South American monsoon system. J Clim 21:6227–6246
Reynolds RW (1988) A real-time global sea surface temperature analysis. J Clim 1:75–86
Ruiz-Barradas A, Nigam S, Karvada A (2014) The Atlantic Multidecadal Oscillation in twentieth century climate simulations: uneven progress from CMIP3 to CMIP5. Clim Dyn. doi:10.1007/s00382-013-1810-0
Santer BD et al (2000) Statistical significance of trends and trend differences in layer-average atmospheric temperature time series. J Geophys Res 105(6):7337–7356
Sarkar S, Singh RP, Kafatos M (2004) Further evidences for the weakening relationship of Indian rainfall and ENSO over India. Geophys Res Lett 31:L13209. doi:10.1029/2004GL020259
Schubert SD, Suarez MJ, Pegion PJ, Koster RD, Bacmeister JT (2004) On the cause of the 1930s dust bowl. Science 303:1855–1859
Schubert SD et al (2009) A USCLIVAR project to assess and compare the responses of global climate models to drought related SST forcing patterns: overview and Results. J. Clim 22:5251–5272
Seager R, Harnik N, Robinson WA, Kushnir Y, Ting M, Huang HP, Velez J (2005) Mechanisms of ENSO-forcing of hemispherically symmetric precipitation variability. Q J R Meteorol Soc 131:1501–1527
Sen PK (1968) Estimates of the regression coefficient based on Kendall's Tau. Am Stat Assoc J 63:1379–1389
Seth A, Rojas M, Rauscher SA (2010) CMIP3 projected changes in the annual cycle of the South American monsoon. Clim Change 98:331–357
Seth A, Rauscher SA, Biasutti M, Giannini A, Camargo SJ, Rojas M (2013) CMIP5 projected changes in the annual cycle of precipitation. J Clim 26:7328–7351. doi:10.1175/JCLI-D-12-00726.1
Silva VB, Kousky SVE, Shi W, Higgins RW (2007) An improved gridded historical daily precipitation analysis for Brazil. J Hydrometeorol 8:847–861
Stensrud DJ, Gall RL, Mullen SL, Howard KW (1995) Model climatology of the Mexican monsoon. J Clim 8:1775–1794
Ting M, Kushnir Y, Seager R, Li C (2009) Forced and internal twentieth century SST trends in the North Atlantic. J Clim 22:1469–1481
Trenberth KE, Stepaniak DP, Caron JM (2000) The global monsoon as seen through the divergent atmospheric circulation. J Clim 13:3969–3993
Vera CS, Silvestri GE, Barros VR, Carril AF (2004) Differences in El Niño response over the Southern hemisphere. J Clim 17:1741–1753
Vera C et al (2006) Toward a unified view of the American monsoon systems. J Clim 19:4977–5000
Vera C, Goswami BN, Gutowski W, Hendon H, Hewitson B, Jones C, Lionello P, Marengo JA, Mechoso R, Reason C, Thorncroft CD (2013) Understanding and predicting climate variability and change at regional scales. In: Asrar GR, Hurrell JW (eds) Climate science for serving society: research, modeling and prediction priorities. Springer, Berlin, pp 273–306
Wang H, Fu R (2002) Cross-equatorial flow and seasonal cycle of precipitation over South America. J Clim 15:1591–1608
Wang C, Lee SK, Enfield DB (2007) Impact of the Atlantic warm pool on the summer climate of the western hemisphere. J Clim 20:5021–5040
Yeh S-W, Kug J-S, Dewitte B, Kwon M-H, Kirtman BP, Jin F-F (2009) El Niño in a changing climate. Nature. doi:10.1038/nature08316
Yeh S-W, Ham J-G, J-Y Lee B (2012) Changes in the tropical Pacific SST trend from CMP3 to CMP5 and its implication of ENSO. J Clim 25(21):7764–7771
Yin L, Fu R, Zhang Y-F, Arias PA, Fernando DN, Li W, Fernandes K, Bowerman AR (2014) What controls the interannual variation of the wet season onsets over the Amazon? J Geophys Res Atmos 119:2314–2328. doi:10.1002/2013JD021349
Zhang R (2007) Anticorrelated multidecadal variations between surface and subsurface tropical North Atlantic. Geophys Res Lett. doi:10.1029/2007GL030225
Zhou J, Lau K-M (1998) Does a monsoon climate exist over South America? J Clim 11:1020–1040
Zhu C, Cavazos T, Lettenmaier DP (2007) Role of antecedent land surface conditions in warm season precipitation over northwestern Mexico. J Clim 20:1774–1791